Title: The ZrfC alkaline zinc transporter is required for *Aspergillus fumigatus* virulence and its growth in the presence of the Zn/Mn-chelating protein calprotectin

Authors: Jorge Amich[1,3], Rocío Vicentefranqueira[1], Emilia Mellado[2], Ana Ruiz-Carmuega[1], Fernando Leal[1] and José Antonio Calera[1]*

Running title: Zinc and virulence in *Aspergillus fumigatus*

Affiliation and present address of authors:

[1]Instituto de Biología Funcional y Genómica (IBFG) (centro mixto del Consejo Superior de Investigaciones Científicas y Universidad de Salamanca) and Departamento de Microbiología y Genética (Universidad de Salamanca). Edificio IBFG, Lab. P1.10. C/ Zacarías González nº 2. 37007 Salamanca, Spain.

[2]Centro Nacional de Microbiología. Instituto de Salud Carlos III. Servicio de Micología. Ctra. Majadahonda-Pozuelo Km 2. 28220 Majadahonda, Madrid, Spain.

[3]Present address, IZKF Forschergruppe für Experimentelle Stammzelltransplantation. Medizinische Klinik und Poliklinik II & Universitäts-Kinderklinik. ZEMM - Zinklesweg 10. 97078 Würzburg, Germany.

***Corresponding author**: Instituto de Biología Funcional y Genómica (IBFG), Lab. P1.10. C/ Zacarías González nº 2. 37007 Salamanca, Spain.

Tel. 34-923-294891; Fax 34-923-224876

e-mail: jacalera@usal.es

ABSTRACT

Aspergillus fumigatus can invade the lungs of immunocompromised individuals causing a life-threatening disease called invasive pulmonary aspergillosis (IPA). To grow in the lungs, *A. fumigatus* obtains from the host all nutrients, including zinc. In living tissues, however, most zinc is tightly bound to zinc-binding proteins. Moreover, during infection the bioavailability of zinc can be further decreased by calprotectin, an antimicrobial Zn/Mn-chelating protein that is released by neutrophils in abscesses. Nevertheless, *A. fumigatus* manages to uptake zinc from and grow within the lungs of susceptible individuals. Thus, in this study we investigated the role of the *zrfA*, *zrfB* and *zrfC* genes, encoding plasma membrane zinc transporters, in *A. fumigatus* virulence. We showed that *zrfC* is essential for virulence in the absence of *zrfA* and *zrfB*, which contribute to fungal pathogenesis to a lesser extent than *zrfC* and are dispensable for virulence in the presence of *zrfC*. The special ability of ZrfC to scavenge and uptake zinc efficiently from lung tissue depended on its N-terminus, which is absent in the ZrfA and ZrfB transporters. In addition, under Zn- and/or Mn-limiting conditions *zrfC* enables *A. fumigatus* to grow in the presence of calprotectin, which is detected in fungal abscesses of non-leucopenic animals. This study extends our knowledge about the pathobiology of *A. fumigatus* and suggests that fungal zinc uptake could be a promising target for new antifungals.

INTRODUCTION

Aspergillus fumigatus is a saprophytic filamentous fungus that can invade the lungs of immunocompromised individuals and cause invasive pulmonary aspergillosis (IPA) (Kousha *et al*., 2011). This fungus exhibits several traits that enable it to grow within living tissues of immunosuppresed patients and cause disease (Tekaia and Latge, 2005; Askew, 2008; Dagenais and Keller, 2009), including its ability to obtain essential cations such as iron and zinc from the hostile environment provided by the host (Calera and Haas, 2009).

The concentration of readily available zinc (i.e. free Zn^{2+} ions) is strongly dependent on the environmental pH as it tends to form complexes with other compounds as pH increases (Sandrin and Maier, 2003). Therefore, the concentration of free Zn^{2+} ions in living tissues at the physiological pH (~ 7.3-7.4) is very low because most zinc is tightly bound to zinc-binding proteins both inside the cells and in extracellular fluids. For instance, the average concentration of total zinc in the human serum is around 15 μM (equivalent to ~ 1 μg per gram of serum) (Iyengar and Woittiez, 1988). However, most zinc in serum is bound to plasma zinc-binding proteins such as albumin and α_2-macroglobulin (Foote and Delves, 1984). Thus, the average concentration of free Zn^{2+} in serum is 0.08 μM (~ 5 ng/g) (Foote and Delves, 1988), which is about 150-fold lower than the minimal concentration required for *A. fumigatus* to grow optimally in a defined liquid medium (unpublished data).

The average concentration of total zinc in human lungs is around 12 μg per gram of lung tissue (Lech and Sadlik, 2011) but the concentration of free Zn^{2+} in the lungs has not been reported. Nevertheless, given that lungs have an extensive network of vessels and capillaries, the concentration of free Zn^{2+} in the extracellular fluid of the lungs should be similar to that in serum. In addition, the zinc availability during fungal invasion could be reduced further in lung abscesses by calprotectin, which is a Zn/Mn-chelating protein released by neutrophils that is

able to inhibit microbial growth by sequestering Zn^{2+} and Mn^{2+} (Korndörfer *et al*., 2007; Corbin *et al*., 2008; Hayden *et al*., 2013). Thus far, it has not been reported whether calprotectin is able to inhibit the growth of *A. fumigatus* although it can inhibit the growth of other fungi such as *Candida albicans* (Steinbakk *et al.*, 1990; Sohnle *et al.*, 1996; Urban *et al.*, 2009) and *A. nidulans* (Bianchi *et al.*, 2011). In sum, both healthy and infected lung tissues provide a slightly alkaline zinc-limiting environment that prevents any sustained microbial growth unless microorganisms had developed some mechanisms to circumvent this nutritional restriction at the pH of the lungs.

The adaptation of *A. fumigatus* to grow in the lungs under alkaline zinc-limiting conditions is co-regulated by the ZafA and PacC transcription factors, which are essential for *Aspergillus* virulence (Bignell *et al*., 2005; Moreno *et al*., 2007). PacC adjusts to the environmental pH the induction of zinc uptake by ZafA under zinc-limiting conditions (Moreno *et al*., 2007; Amich *et al*., 2009; Amich *et al*., 2010). Thus, when Δ*zafA* conidia germinate on the lung mucous membrane produce short germ tubes that stop growing soon afterwards because they cannot express any zinc uptake system (Moreno *et al*., 2007).

The most obvious downstream target genes of ZafA that primarily would determine the virulence of *A. fumigatus* should be those involved in zinc uptake through the plasma membrane. In eukaryotic cells the transport of zinc from the extracellular space (or organellar lumen) into the cytoplasm relies on proteins belonging to the Zrt-, Irt-like Protein (ZIP) family of zinc transporters (Gaither and Eide, 2001). Six ZIP transporters of the eight encoded by the *A. fumigatus* genome (*zrfA, zrfB, zrfC, zrfD, zrfE* and *zrfH*) are localized presumably at the plasma membrane (Calera and Haas, 2009). The transcription levels of the *zrfD*, *zrfE* and *zrfH* genes are similar in acidic and alkaline media regardless of zinc availability and are not regulated by ZafA (unpublished data). In contrast, the expression of the *zrfA*, *zrfB* and *zrfC* genes is up-regulated by ZafA only under zinc-limiting conditions (Vicentefranqueira *et al*.,

2005; Amich *et al*., 2009; Amich *et al*., 2010). Therefore, the capacity of *A. fumigatus* hyphae to scavenge and uptake zinc from the lung mucosa and abscesses could rely on the function of these genes, which hence might be critical for fungal virulence.

In this work we investigated the role of the *zrfA*, *zrfB* and *zrfC* genes in the pathobiology of *A. fumigatus*. We found that ZrfC was the major zinc transporter devoted to scavenge and uptake zinc from living tissues. This capacity of ZrfC was largely dependent on its N-terminus, which is absent in the ZrfA and ZrfB transporters. Besides, under Zn- and/or Mn-limiting conditions *zrfC* enables *A. fumigatus* to overcome the Zn/Mn-chelating capacity of calprotectin, which is readily detected in fungal abscesses of non-leucopenic animals. These findings suggested that *zrfC* might confer *A. fumigatus* the capacity to grow in the alkaline zinc-limiting environment provided by the lung tissue and/or abscesses of immunosupressed individuals with IPA.

RESULTS

ZrfC is the major zinc transporter used by *A. fumigatus* to obtain zinc from host tissue

The ZafA regulator induces the transcription of the *zrfA* and *zrfB* genes at the highest level under acidic zinc-limiting conditions, whereas under neutral and alkaline zinc-limiting conditions their expression is remarkably reduced (Vicentefranqueira *et al*., 2005). In spite of this, the expression level of both genes in alkaline zinc-limiting conditions could be high enough to play a role in pathogenesis. In contrast, ZafA induces the *zrfC* transcription exclusively under alkaline and extreme zinc-limiting conditions (Amich *et al*., 2010). To determine the relevance of all these genes in the pathobiology of *A. fumigatus*, the survival of non-leucopenic mice (NL-mice), was analyzed in parallel with that of leucopenic mice (L-mice) inoculated with the wild-type, Δ*zrfC*, Δ*zrfABC* or Δ*zrfABC*[*zrfC*] strains using 10^5 conidia per mouse (c/m) **(Fig. 1)**. In both murine models of IPA, the survival rates of mice inoculated with the Δ*zrfC* mutant (45% in NL-mice and 23.8% in L-mice) were significantly higher than those of mice inoculated with the wild-type (AF54 > AF14), i.e. the deletion of *zrfC* significantly reduced the virulence of *A. fumigatus* ($P < 0.0001$). This reduction in virulence further increased in a Δ*zrfAB* background. Thus, the survival rates of NL- and L-mice inoculated with a Δ*zrfABC* strain were 100% and 76.9%, respectively. In both murine models of IPA the virulence of the Δ*zrfABC* strain was restored at the wild-type level upon reintroduction of the *zrfC* gene (i.e. a Δ*zrfABC*[*zrfC*] strain showed a wild-type virulence). In concordance with this, a Δ*zrfAB* strain exhibited a wild-type virulence similar to that of a Δ*zrfABC*[*zrfC*] strain, as shown in an independent bioassay in L-mice **(Fig. S1)**. All these results indicated that the *zrfC* gene was essential for virulence in the absence of the *zrfA* and *zrfB* genes, whereas these genes were dispensable for virulence in the presence of *zrfC*. Therefore, *zrfA* and *zrfB* have an accessory

role in virulence to that of *zrfC*. Intriguingly, the deletion of *zrfC* seemed to reduce fungal virulence at a larger extent in NL- than in L-mice, which suggests that NL-mice somehow pose a more restricted environment regarding zinc availability.

Histological examinations of lung sections from L-mice inoculated with the wild-type and Δ*zrfABC*[*zrfC*] strains revealed a high degree of invasion around the lung airways, with hyphae that spread throughout the lung parenchyma and angioinvasion **(Fig. 2, right panels)**. The lung tissue surrounding the affected areas was characterized by oedema and intra-alveolar haemorrhage. The great structural disorganization of the lung tissue caused by the fungal overgrowth might explain the sudden decrease in survival of L-mice inoculated with wild-type and Δ*zrfABC*[*zrfC*] strains between 4 and 5 days post-infection. In contrast, the lung sections of L-mice inoculated with the Δ*zrfC* strain showed a paucity of conspicuous, clearly defined oedematous and necrotized areas with a low degree of fungal invasion and tissue damage. The lungs of L-mice inoculated with the Δ*zrfABC* strain showed a very low degree of fungal invasion. Nevertheless, germinated Δ*zrfABC* conidia were readily observed on the epithelia of the lung airways and within macrophages. The histopathological findings and the fungal burden of L-mice inoculated with each *A. fumigatus* strain correlated well with the survival rates **(Table 1)**. Unlike L-mice, lung sections from NL-mice inoculated with the wild-type, Δ*zrfC* or Δ*zrfABC*[*zrfC*] strain showed well defined infectious foci infiltrated with neutrophils and the absence of angioinvasion **(Fig. 2, left panels)**. The infectious foci produced by the Δ*zrfC* strain showed a degree of fungal growth and neutrophil infiltration much lower than those produced by the wild-type and Δ*zrfABC*[*zrfC*] strains. Mice sacrificed after 15 days post-infection with the Δ*zrfABC* strain showed weak signs of an inflammatory response and very few germinated conidia. The low fungal burden of the Δ*zrfABC* strain in the lungs is unlikely to be due to a defect in germination as the *zrfA, zrfB* and *zrfC* genes were not required for germination *in vitro* under alkaline zinc-limiting conditions **(Fig. S2)**. However, the Δ*zrfC* and Δ*zrfABC* strains

showed a defect in their capacities to grow onto the same media without a zinc supplement and solidified with agar, i.e. the SDN alkaline zinc-limiting and the BSD50 bovine serum agar media **(Fig. S3)**. Taken these results together, it was concluded that the low fungal burden of the Δ*zrfC* and Δ*zrfABC* strains in the lungs of immunosuppressed animals arises from a zinc shortage caused by a defect in zinc uptake during fungal growth, which slows down the growth of the Δ*zrfC* mutant and stops that of the Δ*zrfABC* germ tubes, as reported previously for a Δ*zafA* mutant (Moreno et al., 2007). In summary, the histopathological analysis of lungs from both L- and NL-mice were consistent with survival data and the relevance of the *zrfA*, *zrfB* and *zrfC* genes in the virulence of *A. fumigatus*.

The N-terminus of ZrfC is required for zinc uptake from the lung tissue

The *zrfC* gene plays a role more relevant for *A. fumigatus* virulence than the *zrfA* and *zrfB* genes. However, this was not unexpected because under alkaline zinc-limiting culture conditions (similar to that provided by the lung tissue) the expression of *zrfC* is higher than that of *zrfA* and *zrfB* (Amich *et al*., 2009; Amich *et al*., 2010). Thus, to investigate if the transcriptional profiles of these genes explained their different relevance in virulence, we exchanged the coding sequences between the *zrfC* and *zrfB* genes and analysed the growth capacity of fungal strains expressing the chimerical $zrfB^{P}\rightarrow zrfC^{cds}$ and $zrfC^{P}\rightarrow zrfB^{cds}$ genes in a Δ*zrfABC* background **(Fig. 3A)**. The transcription of these chimerical genes occurred as expected, i.e. *zrfC* expressed at its highest level under acidic conditions and at a lesser extent under alkaline conditions whereas *zrfB* only expressed in the alkaline medium **(Fig. 3B)**. The expression of $zrfB^{cds}$ driven by $zrfC^{P}$ and the expression of $zrfC^{cds}$ driven by $zrfB^{P}$ did not enhance the fungal growth capacity under acidic zinc-limiting conditions **(Fig. 3C)**. The growth capacity of a strain that expresses $zrfC^{cds}$ driven by $zrfB^{P}$ was reduced drastically under alkaline zinc-limiting conditions

compared to that of a strain expressing the wild-type *zrfC* gene **(Fig. 3C)**. In contrast, the growth ability of a strain that expresses $zrfB^{cds}$ driven by $zrfC^{P}$ was enhanced slightly under alkaline conditions compared to that of a strain that expresses the wild-type *zrfB* gene **(Fig. 3C)**. These results indicated that $zrfC^{cds}$ cannot promote the zinc uptake from acidic media whereas $zrfB^{cds}$ can do so from alkaline media, although less efficiently than from acidic media. Besides, this is in perfect agreement with functional complementation studies of these proteins in a yeast model (Vicentefranqueira *et al.*, 2005; Amich *et al.*, 2010). Therefore, these results predicted that the transcriptional profiles of the *zrfB* and *zrfC* genes *per se* would not be sufficient to explain the profuse fungal growth capacity in the alkaline zinc-limiting environment of the lungs and, hence, in virulence. Consequently, the importance of *zrfC* in virulence should be based on structural features of the ZrfC protein that would enable ZrfC to scavenge and uptake Zn^{2+} specifically under alkaline and extreme zinc-limiting conditions.

The most obvious structural difference between ZrfC and ZrfA/ZrfB is that the former has a long N-terminus (~ 200 residues) with four putative zinc-binding motifs that extends towards the extracellular side of the membrane, which is absent in the ZrfA and ZrfB proteins (Amich *et al.*, 2010). In addition, the growth ability under alkaline zinc-limiting conditions (i.e. with a 0-1 μM Zn^{2+} supplement) of a strain that expresses the $zrfC^{\Delta N}$ gene (i.e. a mutated version of the *zrfC* gene that encodes a ZrfC protein without its N-terminus) was more similar to the growth capacity of a strain that expresses $zrfB^{cds}$ driven by the same promoter (i.e. $zrfC^{P}$) than to that of a strain expressing the wild-type *zrfC* gene **(Fig. S4)**. This indicated that the zinc uptake capacity of the $ZrfC^{\Delta N}$ protein might be more similar to that of the ZrfB protein than to the zinc uptake capacity of the wild-type ZrfC protein and, consequently, that the capacity of ZrfC to enhance both fungal growth under alkaline zinc-limiting conditions and virulence might largely depend on its N-terminus. Therefore, to investigate the role of the N-terminus of ZrfC in virulence, we inoculated leucopenic mice with a $\Delta zrfABC[zrfC^{\Delta N}]$ strain using our standard

inoculum (i.e. 10^5 c/m) and a low-dose inoculum (10^4 c/m) (Smith *et al.*, 1993) **(Fig. 4A)**. At first the use of a low-dose inoculum was primarily intended to detect any unexpected subtle differences in virulence between the Δ*zrfABC*[*zrfC*] and Δ*zrfABC*[$zrfC^{\Delta N}$] strains. Nevertheless, as expected the survival rate of L-mice inoculated with the Δ*zrfABC*[$zrfC^{\Delta N}$] strain was significantly higher than that of mice inoculated with the Δ*zrfABC*[*zrfC*] strain (AF791 > AF731, $P = 0.008$). Interestingly, the survival rate of L-mice inoculated with a Δ*zrfABC*[$zrfC^{\Delta N}$] strain was similar to that of L-mice inoculated with a Δ*zrfC* strain for each inoculum size (i.e. ~50% survival for L-mice inoculated with 10^4 c/m and ~20% for L-mice inoculated with 10^5 c/m). Accordingly, the lung sections from L-mice inoculated with a low-dose inoculum of the Δ*zrfABC* strain appeared healthy whereas that from L-mice inoculated with the Δ*zrfC* and Δ*zrfABC*[$zrfC^{\Delta N}$] strains showed a few number of conspicuous oedematous areas with a lower degree of fungal invasion and tissue damage than mice killed by the wild-type and Δ*zrfABC*[*zrfC*] strains **(Fig. 4B)**. In summary, these results indicated that ZrfC without its N-terminus has lost its ability to scavenge and uptake zinc from living tissue as efficiently as the native ZrfC protein. In addition, the nearly identical survival rates of L-mice inoculated with the Δ*zrfC* and Δ*zrfABC*[$zrfC^{\Delta N}$] strains pointed out that the zinc uptake activity of ZrfC without its N-terminus (in the Δ*zrfABC*[$zrfC^{\Delta N}$] strain) should equal that of the ZrfA and ZrfB together (in the Δ*zrfC* strain).

zrfC enables *A. fumigatus* to overcome the effect of calprotectin under Mn- and/or Zn-limiting conditions

Calprotectin is a Zn/Mn-chelating protein with antimicrobial properties that is released by infiltrated neutrophils in abscesses (Corbin *et al*., 2008). As shown before, NL-mice inoculated with the wild-type, Δ*zrfC* or Δ*zrfABC*[*zrfC*] strain showed well defined infectious foci infiltrated with neutrophils whereas L-mice did not show obvious neutrophil infiltrations **(Fig. 2)**. Thus, it would be expected that the amount of calprotectin released by neutrophils around or within the infectious foci of L-mice were lower than that released in fungal abscesses of NL-mice. Indeed, we showed by immunocytochemistry (using an antibody raised against the calgranulin A subunit of mouse calprotectin) that calprotectin was detected in patches that localized coordinately with fungal abscesses in lung sections of NL-mice infected with a Δ*zrfABC*[*zrfC*] strain **(Fig. 5, left I panels)**. In contrast, calprotectin was localized in scattered neutrophils throughout the whole lung sections of infected L-mice **(Fig. 5, right I panels)**. As expected, the lung sections of non-inoculated NL-mice showed an amount of calprotectin (observed within neutrophils) >10-fold higher than the non-inoculated L-mice ($P > 0.0001$) **(Fig. 5, NI panels)**. The comparison of the increase rates in the amount of calprotectin between lung sections of non-inoculated and inoculated mice revealed surprisingly that the lung calprotectin content increases at a lesser extent in infected NL-mice (~ 12-fold) than in infected L-mice (~ 28-fold). Nevertheless, the gross amount of calprotectin in lung sections of NL-mice was significantly higher than that of L-mice infected with a Δ*zrfABC*[*zrfC*] strain (~ 5.6-fold; $P = 0.0002$) **(Fig. 5)**. Therefore, given that the Δ*zrfC* and Δ*zrfABC* strains were less virulent in NL-mice than in L-mice and that the zinc transporter ZrfC is required for *A. fumigatus* to grow in living tissues, we wondered whether the *zrfC* gene enables *A. fumigatus* to grow in the presence of calprotectin (as it might occur in the fungal abscesses of NL-mice). Thus, we

performed microculture-based bioassays for all strains in an alkaline Mn-replete but Zn-limiting medium (pH 7.2) in the presence of 2.0 μM recombinant human calprotectin (rhCP) to investigate the effect of calprotectin on the growth of *A. fumigatus* **(Fig. 6A)**. Under these cultures conditions calprotectin inhibited significantly the growth capacity of the Δ*zrfC* strain (P = 0.0092), which showed a 2.6-fold reduction compared with the growth capacity in the absence of calprotectin **(Fig. 6A, left panel)**. The growth capacity of the Δ*zrfABC* strain was not inhibited by calprotectin and was similar to that of the Δ*zrfC* strain in presence of calprotectin. The addition of a Zn^{2+} supplement not only increased the growth capacity of all strains but also suppressed the effect of calprotectin on the growth of the Δ*zrfC* strain **(Fig. 6A, right panel)**. This indicated that the *zrfC* gene (but not the *zrfA* and *zrfB* genes) was able to counteract completely the inhibition of fungal growth by calprotectin under Zn-limiting conditions.

Additionally, given that calprotectin also binds manganese (Hayden *et al*., 2013), we also tested whether the *zrfC* gene was able to counteract the inhibition of fungal growth by calprotectin under Mn- and Zn-limiting conditions **(Fig. 6B)**. Thus, we observed that calprotectin reduced by 2.2-fold the growth capacity of the wild-type strain and nearly abrogated the fungal growth capacity of a Δ*zrfC* null mutant **(Fig. 6B, left panel)**. The addition of Zn^{2+} increased the overall growth capacity of all strains and suppressed completely the antifungal effect of calprotectin against the wild-type and Δ*zrfAB*[*zrfC*] strains **(Fig. 6B, right panel)**. In contrast, a Zn^{2+} supplement did not restored completely the growth capacity of the Δ*zrfC* strain. This unexpected finding suggested that *zrfC* might play also a role in overcoming the effect of calprotectin under Mn-limiting conditions. However, under zinc-limiting conditions the Δ*zrfC* strain grew identical on both Mn-limiting and Mn-replete agar **(Fig. S5)**. Therefore, if the ZrfC transporter is involved in manganese uptake under Zn-limiting conditions its overall contribution to this process must be very low. Lastly, we observed that the addition

of Zn^{2+} and Mn^{2+} to Δ*zrfC* microcultures after 60 hours of incubation in the presence of calprotectin restored the growth capacity of the Δ*zrfC* strain as in the absence of rhCP (P = 0.001). This indicated that calprotectin had a fungistatic effect against this strain (data not shown).

In summary, under the Mn- and Zn-limiting conditions used in our experiments the growth capacity of a wild-type strain of *A. fumigatus* was reduced about 50% in the presence of calprotectin compared to in the absence of calprotectin. However, the *zrfC* gene (but not *zrfA* and *zrfB* genes) enables *A. fumigatus* to overcome partially the static effect of calprotectin on fungal growth under Mn- and Zn-limiting conditions, but completely under either Mn- or Zn-limiting conditions.

DISCUSSION

One of the most critical aspects for pathogens to grow in a susceptible organism and cause disease is their ability to uptake nutrients from the host tissues. In this regard, we reported for the first time that the regulation of zinc homeostasis by the ZafA transcriptional regulator was essential for virulence in the pathogenic fungus *A. fumigatus* (Moreno *et al*., 2007). In addition, in a previous work we anticipated that the *zrfC* gene of *A. fumigatus*, which encode a new prototype of ZIP transporters exclusively distributed among fungi (Amich *et al*., 2010), could be the main responsible for zinc uptake from host tissues. This assumption was based on two facts: (i) the *zrfC* gene is up-regulated by the essential-for-virulence ZafA transcriptional activator exclusively under alkaline zinc-limiting conditions (i.e. that provided by host tissues); (ii) ZrfC has a long N-terminus towards the extracellular side of the plasma membrane that could be use for scavenging Zn^{2+} from the lungs. In addition, the *zrfA* and *zrfB* genes could play a role in *A. fumigatus* virulence as they both are also up-regulated by ZafA under alkaline zinc-limiting conditions, although at a lesser extent than in acidic zinc-limiting media (Vicentefranqueira *et al*., 2005). Nevertheless, the relevance of ZafA target genes that encode specific zinc transporters in fungal virulence remained to be proven. Therefore, we analysed the role of these genes in fungal virulence using mice subjected to both a leucopenic and non-leucopenic immunosuppresive regime that resemble those most frequently administered to patients at a highest risk of IPA. In addition, we also intended to ascertain whether the role of these genes in virulence was influenced by the immunosuppressive regime, as it may determinate the pathobiology of *A. fumigatus* (Spikes *et al.*, 2008; Kwon-Chung and Sugui, 2009) and the development, pathogenesis and histopathology of IPA (Berenguer *et al*., 1995; Balloy *et al*., 2005; Stephens-Romero *et al*., 2005). However, both murine models of IPA essentially raised the same conclusion about the role of these genes in the pathobiology of *A.*

fumigatus, i.e. ZrfC is the major ZIP transporter used by *A. fumigatus* to uptake zinc from the lungs whereas ZrfA and ZrfB have an accessory although relevant role to fulfil the nutritional requirement of *A. fumigatus* growing in the lungs and, hence, in virulence. This conclusion is supported by the fact that the deletion of the *zrfA* and *zrfB* genes is compensated completely by *zrfC* (in the Δ*zrfAB* and Δ*zrfABC*[*zrfC*] strains) whereas the deletion of *zrfC* is compensated partially by *zrfA* and *zrfB* (in a Δ*zrfC* strain). Indeed, the expression of the ZrfC transporter, which is adapted to function under alkaline conditions (Amich *et al.*, 2010), might easily overcome the lack of the ZrfA and ZrfB transporters in the former strains. In contrast, it would be expected that the expression of the ZrfA and ZrfB transporters, which are adapted to uptake zinc from acidic media more efficiently than from alkaline media (Amich *et al.*, 2010), is largely insufficient to compensate the absence of ZrfC in a Δ*zrfC* strain. However, a Δ*zrfC* strain is more virulent than expected if the *zrfA* and *zrfB* genes are dispensable for virulence, as shown. In this regard, we hypothesized that the attenuated virulence of a Δ*zrfC* strain could be due to an increase in the transcription level of *zrfA* and/or *zrfB* as part of a compensatory mechanism to alleviate the zinc shortage of this strain growing under the alkaline and extreme zinc-limiting conditions provided by the lung tissue. To test this hypothesis we measured and compared the transcription level of the *zrfA* and *zrfB* genes between the Δ*zrfC* and wild-type strain both grown *in vitro* under alkaline and extreme zinc-limiting conditions **(Fig. S6)**. Interestingly, we showed that in a Δ*zrfC* background the expression of *zrfA* and *zrfB* increases approximately by 3.5 and 2-fold, respectively, compared to a wild-type strain. This finding is consistent with the notion that the attenuated virulence of a Δ*zrfC* strain might be due to the overexpression of their *zrfA* and *zrfB* genes when growing in the zinc-limiting environment of the lungs.

The special ability of ZrfC to function under alkaline zinc-limiting conditions largely depends on its N-terminus, which is absent in the acidic zinc transporters (ZrfA and ZrfB). Indeed, the $ZrfC^{\Delta N}$ protein enhances cell growth in a yeast model at a similar extent than the

ZrfA and ZrfB proteins under alkaline zinc-limiting conditions (Amich *et al.*, 2010). In addition, the N-terminus of ZrfC is required for virulence, which is consistent with the notion that the N-terminus of ZrfC could function in Zn^{2+} scavenging from host tissues. Moreover, it could function in Zn^{2+} scavenging in concert with other proteins such as Aspf2, which is an immunodominant antigen secreted by *A. fumigatus* (Banerjee *et al.*, 1998; Segurado *et al.*, 1999) that could bind zinc and whose expression is also up-regulated by ZafA (Amich *et al.*, 2010). In this regard, a similar mode of action has been proposed for the Pra1 and Zrt1 proteins of *Candida albicans* (Citiulo *et al.*, 2012), which are the Aspf2 and ZrfC orthologues, respectively. However, the deletion of *zrfC* does not influence the *aspf2* expression and the deletion of *aspf2* has no impact either on the *zrfC* expression or *A. fumigatus* virulence (unpublished data). Thus, further investigations will be required to establish the relevance of a putative ZrfC-Aspf2 interaction in the ZrfC and/or Aspf2 functionality and its connection to the pathobiology of *A. fumigatus*.

Calprotectin is a heterodimeric protein synthesized constitutively at high levels by neutrophils (Striz and Trebichavsky, 2004). It binds two metal ions (either 2 Zn^{2+} or 1 Zn^{2+} plus 1 Mn^{2+}) with high affinity (Korndörfer *et al.*, 2007; Hayden *et al.*, 2013), which may deplete zinc and manganese in culture media and, in turn, inhibit microbial growth *in vitro* (Steinbakk *et al.*, 1990; Miyasaki *et al.*, 1993; Sohnle *et al.*, 1996; Sohnle *et al.*, 2000; Corbin *et al.*, 2008; Bianchi *et al.*, 2011; Liu *et al.*, 2012). To inhibit microbial growth *in vivo* calprotectin is released in abscesses by neutrophils through the formation of neutrophil extracellular traps (NETs) (Fuchs *et al.*, 2007; Urban *et al.*, 2009). Like most pathogens, *Aspergillus* also triggers the release of NETs by neutrophils both *in vitro* and *in vivo* (Bruns *et al.*, 2010; McCormick *et al.*, 2010; Bianchi *et al.*, 2011). However, so far it has not been proven whether calprotectin inhibits the growth of *A. fumigatus* as it does that of *A. nidulans* (Bianchi *et al.*, 2011). Here we show that calprotectin does inhibit the growth capacity of *A. fumigatus in vitro* and that *zrfC*

enables the fungus to overcome the effect of calprotectin under Zn- and/or Mn-limiting conditions. However, there are some striking differences between the effect of calprotectin on the growth of *A. fumigatus* and that reported for *A. nidulans*. For instance, a supplement of Mn^{2+} suppresses the effect of calprotectin against *A. fumigatus* but not against *A. nidulans* (Bianchi *et al.*, 2011). Additionally, calprotectin has a fungistatic effect on a Δ*zrfC* strain of *A. fumigatus* at a concentration of 2 μM (equivalent to 57.3 μg/mL) whereas it has a fungicidal effect on a wild-type strain of *A. nidulans* at a concentration of 16 μg/mL (Bianchi *et al.*, 2011). These data suggest that *A. nidulans* may exhibit a susceptibility to calprotectin higher than *A. fumigatus*. Interestingly, this could be explained in terms of a lower Zn^{2+} scavenging capacity of the *A. nidulans* ZrfC-like protein, which has a shorter N-terminus with one less putative zinc-binding motif than the ZrfC protein from *A. fumigatus* (data not shown). However, it is also possible that the different susceptibility of these fungi to calprotectin could be explained by the distinct culture conditions and/or experimental procedures used for the *in vitro* bioassays.

An unexpected finding of this work is that the ZrfC transporter could play also a role in manganese uptake under Mn-limiting conditions. In this regard, it is worth noting that some ZIP proteins of the LZT family (Taylor and Nicholson, 2003), also characterized by having a long extracellular N-terminus similar to ZrfC, have been reported to uptake both Zn^{2+} and Mn^{2+} (Himeno *et al.*, 2009). Moreover, given the importance of Mn^{2+} for oxidative stress management, it is tempting to speculate about a role of ZrfC in manganese uptake as a mechanism to counteract the increase in ROS production under the extreme Zn-limiting conditions imposed by calprotectin (Jakubovics *et al.*, 2002; Kehl-Fie *et al.*, 2011).

Many different physiological aspects from both the host and fungus determine the development and pathophysiology of IPA. For instance, NL-mice show an exacerbated and sustained inflammatory response to *A. fumigatus* hyphae compared to L-mice (Balloy *et al*., 2005). This response may prevent fungal invasion in NL-mice, e.g. through the formation of

NETs (Bruns *et al.*, 2010; McCormick *et al.*, 2010), but causes a respiratory distress that may lead to death (Balloy *et al*., 2005). We have observed that, in terms of survival, the deletion of *zrfC* seemed to reduce fungal virulence at a larger extent in NL- than in L-mice. This observation led us to postulate that calprotectin released by neutrophils in fungal abscesses of NL-mice may create extremely Zn- and Mn-limiting microenvironments. In these conditions, the fungus could manage to grow using the ZrfC protein for Zn^{2+} scavenging and uptake by overcoming the Zn/Mn-chelating activity of calprotectin. In contrast, the low amount (or complete absence) of calprotectin released in the infectious foci of L-mice would allow the fungus to use ZrfC to uptake zinc more efficiently resulting in a profuse and extended fungal growth. The demonstration of this hypothesis will surely improve our understanding of the IPA pathogenesis. In either case, our findings about the mechanisms used by *A. fumigatus* to obtain zinc from the host expands our knowledge about the pathobiology of *A. fumigatus* and might anticipate the development of new antifungal therapies to treat IPA based on inhibiting fungal zinc uptake.

EXPERIMENTAL PROCEDURES

Strains, growth media and culture conditions

All fungal strains used in this work are listed in **Table 2**. All strains were routinely grown in PDA complex medium (20 g/L potato dextrose agar, 20 g/L sucrose, 2.5 g/L $MgSO_4.7\ H_2O$, 1 m/L Hutner's trace element solution 1000×) (Amich *et al*., 2009).

The acidic and alkaline zinc-limiting liquid (SDA–Zn, pH 4.5 and SDN–Zn, pH 7.5) and agar (SDAE–Zn, pH 4.5 and SDNE–Zn, pH 7.5) media were prepared as described previously (Amich *et al.*, 2010). The alkaline BSD10 and BSD50 media (pH 7.5) are complex media than contains 0.1 g/L dextrose and 10% or 50% (v/v) bovine serum (cat. nº 16170-078, Invitrogen). The BSD plates were solidified with 2% agar. The BSD media are not zinc-limiting media as bovine serum usually contains >10 μM zinc (Yokus and Cakir, 2006). Agar media were spotted with 10^3 conidia per strain. Liquid media were inoculated to a density of 5×10^5 spores/mL and incubated at 37°C with shaking at 200 rpm.

The fungal growth capacity in microcultures was tested *in vitro* in the liquid Synthetic Dextrose Nitrate–Zn–Mn medium (SDN–Zn–Mn, pH 7.2) (20 g/L Dextrose, 3 g/L $NaNO_3$, 1 g/L KH_2PO_4, 0.5 g/L $MgSO_4$ - $7H_2O$, 5 mL/L vitamin solution 100× [RPMI-1640, Sigma], 1.0 mL/L YNB–Zn–Mn trace element solution 1000× [50 g/L NaCl, 14.7 g/L $CaCl_2$-2 H_2O, 0.5 g/L BO_3H, 0.1 g/L IK, 1.4 g/L $FeSO_4$ -7 H_2O, 0.4 g/L $CuSO_4$-5 H_2O, 0.72 g/L Na_2MoO_4-2 H_2O]). Media were supplemented with Zn^{2+} and/or Mn^{2+} using sterile stock solutions of 1.0 mM $ZnSO_4.7\ H_2O$ or $MnSO_4.H_2O$ in ultrapure water. The concentration of total zinc and total manganese in the liquid SDN–Zn–Mn medium was 1.15 ± 0.3 μM and 0.8 ± 0.1 μM, respectively, as determined by Inductively Coupled Mass Spectrometry in a Perkin-Elmer Elan

6000 ICP-MS instrument using mineralized samples of this medium and the appropriate standards for calibration.

Standard molecular biology procedures

DNA manipulations were performed following standard molecular biology protocols (Sambrook and Russell, 2001). The transforming DNA used to construct the AF771 and AF781 strains was obtained from plasmids pZRF28 and pZRF310, respectively. The pZRF28 plasmid was designed and constructed to reintroduce the coding sequence of *zrfB* under the control of the *zrfC* promoter at the *pyrG* locus of the *A. fumigatus* AF2511 strain. More precisely, the chimerical $zrfC^{P} \rightarrow zrfB^{cds}$ gene was targeted at few nucleotides downstream from the $pyrG^{cds}$ 3'-end in the intergenic region between the AFUA_2G08360 (*pyrG*) and AFUA_2G08350 loci. A NheI/HpaI fragment from plasmid pZHA2, which carries the *zrfB* coding sequence, was ligated to the pPYRGQ5 plasmid to generate the pZRF28 plasmid. The pZRF310 plasmid was also constructed to reintroduce the coding sequence of *zrfC* under the control of the *zrfB* promoter at the *pyrG* locus of the AF2511 strain. A BglII/HpaI fragment from plasmid pZRF39, which carries the *zrfC* coding sequence, was ligated to the pPYRGQ4 plasmid to generate the pZRF310 plasmid. The pZHA2, pPYRGQ5, pZRF39 and pPYRGQ4 plasmids were constructed as described previously (Amich *et al.*, 2010).

DNA and RNA from *A. fumigatus* were purified and analysed as described previously (Amich *et al.*, 2010). A DNA fragment of 778 bp obtained from the pZRF24g plasmid (Vicentefranqueira *et al.*, 2005) and a DNA fragment of 714 bp obtained from the pZRF30 plasmid (Amich *et al.*, 2010) were used as probes in northern blot for the coding sequences of *zrfB* and *zrfC*, respectively.

Construction of prototrophic and isogenic strains of *A. fumigatus*

The Δ*zrfC* (AF431), Δ*zrfAB* (AF10) and Δ*zrfABC* (AF251) mutant strains used in a previous study (Amich *et al.*, 2010) were non-isogenic to the wild-type strain (AF14) (Vicentefranqueira *et al.*, 2005) with respect to their functional *pyrG* gene, which may reduce their virulence. Thus, to assess the role of the *zrfA, zrfB* and *zrfC* genes in *A. fumigatus* virulence the prototrophic and isogenic Δ*zrfC* (AF54), Δ*zrfAB* (AF48) and Δ*zrfABC* (AF721) strains were constructed to be certain that the virulence of these strain was not influenced by the expression level of the *Aspergillus niger pyrG* gene used as selectable marker and/or the specific activity of the *A. niger* PyrG protein in *A. fumigatus*. To construct these mutant strains, we took advantage that the spontaneous uridine-uracil auxotrophic Δ*zrfC* (AF52), Δ*zrfAB* (AF15) and Δ*zrfABC* (AF2511) mutant strains carried the C756T mutation (*pyrG1*) near the 3' end of the *A. fumigatus pyrG* coding sequence (Weidner *et al.*, 1998), which can be easily repaired to generate prototrophic and isogenic strains suitable for virulence assays in animals, as described previously (Moreno *et al.*, 2007). Thus, protoplast of the uridine-uracil-auxotrophic AF52, AF15 and AF2511 strains were transformed with a 1.09 kbp BamHI-AvrII fragment excised from plasmid pPYRG0 (Moreno et al., 2007) to generate the AF54, AF48 and AF721 strains, respectively. These strains were analysed by southern blot as described in Moreno et al (2007) using the DIG-labelled transforming DNA fragment as probe. The growth patterns of all strains were tested under different zinc-limiting and zinc-replete culture conditions **(Fig. S3)**. In addition, to ensure that the reduced virulence due to the lack of *zrfC* was not due to any undetected mutations introduced at other loci during manipulation, the uridine-uracil auxotrophic Δ*zrfABC* (AF2511) strain was transformed with a DNA fragment that carries the *zrfC* gene to generate a prototrophic and isogenic *zrfC*-reconstituted strain (Δ*zrfABC*[*zrfC*], AF731), as described previously (Amich *et al.*, 2010).

The prototrophic and isogenic *zrfB*-reconstituted strain (Δ*zrfABC*[*zrfB*], AF761) and the *zrfC*$^{\Delta 13\text{-}622}$-reconstituted strain (Δ*zrfABC*[*zrfC*]$^{\Delta N}$, AF791) were constructed as described previously (Amich *et al.*, 2010). The *zrfC*$^{\Delta 13\text{-}622}$ mutant gene encodes a ZrfC protein without its N-terminus (ZrfC$^{\Delta N}$). The AF771 and AF781 strains were constructed respectively by reintroducing the coding sequence of *zrfB* driven by the *zrfC* promoter (*zrfC*^{P} → *zrfB*^{cds}) and the coding sequence of *zrfC* driven by the *zrfB* promoter (*zrfB*^{P} → *zrfC*^{cds}) at the *pyrG* locus of the AF2511 strain by using the same strategy to construct the AF731, AF761 and AF791 strains. Genomic DNA obtained from several independent PyrG^{+} isolates of these strains was analysed by Southern blot to verify that these strains harboured the correct integration event at the expected locus.

Expression, purification and reconstitution of calprotectin

Human calprotectin (hCP) is made up of two proteins (calgranulin A and B) associated non-covalently (Korndörfer *et al*., 2007). To obtain a biologically functional recombinant hCP (rhCP), the hCalA and hCalB polypeptides were expressed in *Escherichia coli* (BL21-DE3) from plasmids pET28-rhCalA and pTAC2-rhCalB. The proteins were purified by affinity to a Ni-NTA resin, concentrated with Amicon Ultra-15 3K units and dialyzed step-wise against the renaturation buffer (100 mM glycine [pH 7.5], 1 mM EDTA, 1 mM EGTA, 2 mM DTT). The purity of the proteins was >98% as assessed by SDS-PAGE.

The rhCP was reconstituted following a denaturing/renaturing step protocol to obtain an heterodimer with identical biophysical properties as calprotectin purified directly from PMNs (Vogl *et al*., 2006). The rhCP solution (28.5 μM) was stored in aliquots at –20ºC in calprotectin buffer (20 mM Tris-HCl [pH 7.5], 50 μM EDTA, 50 μM EGTA, 0.2 mM DTT).

Bioassay of the effect of calprotectin on fungal growth in microcultures

Microcultures were set up in 20-mL screw-top glass vials. The vials were washed thoroughly with ultrapure water and sterilized at 170ºC. To set up a microculture 1.0 mL of the SDN–/+ Zn medium, 0.36 mL of ultrapure sterile water and 0.14 mL of either calprotectin buffer or reconstituted 28.5 μM rhCP solution were added and mixed gently. Each vial was inoculated with 10^6 conidia. For each strain and culture condition three vials were inoculated and incubated unshaken for 60 hours in a humid atmosphere at 37ºC. The mycelium was harvested by filtration through GFC filters, dried at 70ºC and weighted.

Virulence assays

The animals were housed, cared for and used for experimentation in accordance with the current European (Directive 2010/63/EU of the European Parliament and of the Council) and Spanish (BOE-A-2005-17344) animal welfare regulations. All animal experiments were performed according to the CBA PA45_2011-v2 protocol approved by the "Comité de Ética para Investigación y Bienestar Animal" from the Instituto de Salud Carlos III (ISCIII, Spain). This committee did not raise any concerns and approved our study.

SPF-CD1 male mice (~25 g each) were grouped in cohorts of 10 mice. Spores were harvested from PDA plates and washed twice with a saline buffer plus 0.01% Tween-20. Two different immunosuppressive regimens were used: (i) a cyclophosphamide/cortisone-based treatment, which causes a depletion of circulating white blood cells (i.e. a leucopenic regime) and, (ii) a corticosteroid-based treatment (i.e. a non-leucopenic regime). Mice subjected to the leucopenic regime were immunosuppressed on days –3 and –1 before inoculation with cyclophosphamide (150 mg/kg) and cortisone 21-acetate (112 mg/kg). Afterwards only

cyclophosphamide (150 mg/kg) was administered on day +3, +6, +9 and +12 after inoculation. Mice subjected to the non-leucopenic regimen were immunosuppressed on days –3 and –1 with cortisone 21-acetate (380 mg/kg). Later on day +3 it was administered one extra dose of cortisone (190 mg/kg). Before infection, each mouse was anesthetized with 0.1 mL of a mix of ketamine plus xylazine. Each mouse was inoculated intranasally with 30 µL of a suspension with 6.5×10^6 conidia/mL (or 6.5×10^5 conidia/mL) to ensure that during the instillation process each mice is inoculated with no less than 10^5 conidia (or 10^4 conidia). Non-inoculated control immunosuppressed mice only received saline buffer. Mice were euthanized to avoid suffering when they developed symptoms of severe respiratory distress.

Histology and immunocytochemistry

One lung from each mouse was fixed in 10 mL of 10% neutral buffered formalin for 6 hours at room temperature and then transferred to 70% ethanol. Each lung was embedded in paraffin and cut into 4 µm thick sections that were stained with the Grocott's methenamine-silver nitrate (GMS) procedure, followed by a counterstain with H&E (GMS-HE stain) as described elsewhere (Huppert *et al.*, 1978).

To detect calprotectin was used an indirect immunocytochemical method with the avidin-biotin-peroxidase complex procedure (Hsu *et al.*, 1981), using a goat anti-mouse calgranulin A antibody (C1033-50E US Biologicals) or a goat isotype control (Thermo Scientific, cat. 31871) (both at a 1:500 dilution) as the primary antibody and a biotinylated rabbit anti-goat antibody as the secondary antibody.

High quality images of immunostained lung sections taken with a 4× objective were analysed using the ImageJ 1.47v software (http://imagej.nih.gov/ij) to measure the percent area of immunostained calprotectin. The green channel of split images, which provided the best

separation, was used for the threshold process. The lower and upper threshold levels were set respectively at the values of 0 and 130 for all images.

Determination of fungal burden

One lung from each mouse was weighed, homogenized in PBS and filtered through 100 μm Nylon filters. Each homogenate was used to determine the fungal burden by two different procedures: counting the colony-forming units on PDA plates and measuring the amount of galactomannan per gram of lung tissue using a quantitative GM enzyme immunoassay (Platelia™ GM-EIA kit) according to the manufacturer's instructions (Sheppard *et al*., 2006).

REFERENCES

Amich, J., Leal, F., and Calera, J.A. (2009) Repression of the acid ZrfA/ZrfB zinc-uptake system of *Aspergillus fumigatus* mediated by PacC under neutral, zinc-limiting conditions. *Int Microbiol* **12**: 39-47.

Amich, J., Vicentefranqueira, R., Leal, F., and Calera, J.A. (2010) *Aspergillus fumigatus* survival in alkaline and extreme zinc-limiting environments relies on the induction of a zinc homeostasis system encoded by the *zrfC* and *aspf2* genes. *Eukaryot Cell* **9**: 424-437.

Askew, D.S. (2008) *Aspergillus fumigatus*: virulence genes in a street-smart mold. *Curr Opin Microbiol* **11**: 331-337.

Balloy, V., Huerre, M., Latge, J.P., and Chignard, M. (2005) Differences in patterns of infection and inflammation for corticosteroid treatment and chemotherapy in experimental invasive pulmonary aspergillosis. *Infect Immun* **73**: 494-503.

Banerjee, B., Greenberger, P.A., Fink, J.N., and Kurup, V.P. (1998) Immunological characterization of Asp f 2, a major allergen from *Aspergillus fumigatus* associated with allergic bronchopulmonary aspergillosis. *Infect Immun* **66**: 5175-5182.

Berenguer, J., Allende, M.C., Lee, J.W., Garrett, K., Lyman, C., Ali, N.M., *et al*. (1995) Pathogenesis of pulmonary aspergillosis. Granulocytopenia versus cyclosporine and methylprednisolone-induced immunosuppression. *Am J Respir Crit Care Med* **152**: 1079-1086.

Bianchi, M., Niemiec, M.J., Siler, U., Urban, C.F., and Reichenbach, J. (2011) Restoration of anti-*Aspergillus* defense by neutrophil extracellular traps in human chronic granulomatous disease after gene therapy is calprotectin-dependent. *J Allergy Clin Immunol* **127**: 1243-1252 e1247.

Bignell, E., Negrete-Urtasun, S., Calcagno, A.M., Haynes, K., Arst, H.N., Jr., and Rogers, T. (2005) The *Aspergillus* pH-responsive transcription factor PacC regulates virulence. *Mol Microbiol* **55**: 1072-1084.

Bruns, S., Kniemeyer, O., Hasenberg, M., Aimanianda, V., Nietzsche, S., Thywissen, A., *et al*. (2010) Production of extracellular traps against *Aspergillus fumigatus in vitro* and in infected lung tissue is dependent on invading neutrophils and influenced by hydrophobin RodA. *PLoS Pathog* **6**: e1000873.

Calera, J.A., and Haas, H., (2009) Cations (Zn, Fe). In: *Aspergillus fumigatus* and aspergillosis. J.P. LatgéandSteinbach, W.J. (eds). Washington, DC: ASM press, pp. 107-129.

Citiulo, F., Jacobsen, I.D., Miramon, P., Schild, L., Brunke, S., Zipfel, P., *et al*. (2012) *Candida albicans* scavenges host zinc via Pra1 during endothelial invasion. *PLoS Pathog* **8**: e1002777.

Corbin, B.D., Seeley, E.H., Raab, A., Feldmann, J., Miller, M.R., Torres, V.J., *et al*. (2008) Metal chelation and inhibition of bacterial growth in tissue abscesses. *Science* **319**: 962-965.

Dagenais, T.R., and Keller, N.P. (2009) Pathogenesis of *Aspergillus fumigatus* in Invasive Aspergillosis. *Clin Microbiol Rev* **22**: 447-465.

Foote, J.W., and Delves, H.T. (1984) Albumin bound and alpha 2-macroglobulin bound zinc concentrations in the sera of healthy adults. *J Clin Pathol* **37**: 1050-1054.

Foote, J.W., and Delves, H.T. (1988) Determination of non-protein-bound zinc in human serum using ultrafiltration and atomic absorption spectrometry with electrothermal atomisation. *Analyst* **113**: 911-915.

Fuchs, T.A., Abed, U., Goosmann, C., Hurwitz, R., Schulze, I., Wahn, V., *et al*. (2007) Novel cell death program leads to neutrophil extracellular traps. *J Cell Biol* **176**: 231-241.

Gaither, L.A., and Eide, D.J. (2001) Eukaryotic zinc transporters and their regulation. *Biometals* **14**: 251-270.

Hayden, J.A., Brophy, M.B., Cunden, L.S., and Nolan, E.M. (2013) High-affinity manganese coordination by human calprotectin is calcium-dependent and requires the histidine-rich site formed at the dimer interface. *J Am Chem Soc* **135**: 775-787.

Himeno, S., Yanagiya, T., and Fujishiro, H. (2009) The role of zinc transporters in cadmium and manganese transport in mammalian cells. *Biochimie* **91**: 1218-1222.

Hsu, S.M., Raine, L., and Fanger, H. (1981) Use of avidin-biotin-peroxidase complex (ABC) in immunoperoxidase techniques: a comparison between ABC and unlabeled antibody (PAP) procedures. *J Histochem Cytochem* **29**: 577-580.

Huppert, M., Oliver, D.J., and Sun, S.H. (1978) Combined methenamine-silver nitrate and hematoxylin & eosin stain for fungi in tissues. *J Clin Microbiol* **8**: 598-603.

Iyengar, V., and Woittiez, J. (1988) Trace elements in human clinical specimens: evaluation of literature data to identify reference values. *Clin Chem* **34**: 474-481.

Jakubovics, N.S., Smith, A.W., and Jenkinson, H.F. (2002) Oxidative stress tolerance is manganese (Mn(2+)) regulated in *Streptococcus gordonii*. *Microbiology* **148**: 3255-3263.

Kehl-Fie, T.E., Chitayat, S., Hood, M.I., Damo, S., Restrepo, N., Garcia, C., *et al*. (2011) Nutrient metal sequestration by calprotectin inhibits bacterial superoxide defense, enhancing neutrophil killing of *Staphylococcus aureus*. *Cell Host Microbe* **10**: 158-164.

Korndörfer, I.P., Brueckner, F., and Skerra, A. (2007) The crystal structure of the human (S100A8/S100A9)2 heterotetramer, calprotectin, illustrates how conformational changes of interacting alpha-helices can determine specific association of two EF-hand proteins. *J Mol Biol* **370**: 887-898.

Kousha, M., Tadi, R., and Soubani, A.O. (2011) Pulmonary aspergillosis: a clinical review. *Eur Respir Rev* **20**: 156-174.

Kwon-Chung, K.J., and Sugui, J.A. (2009) What do we know about the role of gliotoxin in the pathobiology of *Aspergillus fumigatus*? *Med Mycol* **47 Suppl 1**: S97-103.

Lech, T., and Sadlik, J.K. (2011) Zinc in postmortem body tissues and fluids. *Biol Trace Elem Res* **142**: 11-17.

Liu, J.Z., Jellbauer, S., Poe, A.J., Ton, V., Pesciaroli, M., Kehl-Fie, T.E., *et al*. (2012) Zinc sequestration by the neutrophil protein calprotectin enhances *Salmonella growth* in the inflamed gut. *Cell Host Microbe* **11**: 227-239.

McCormick, A., Heesemann, L., Wagener, J., Marcos, V., Hartl, D., Loeffler, J., *et al*. (2010) NETs formed by human neutrophils inhibit growth of the pathogenic mold *Aspergillus fumigatus*. *Microbes Infect* **12**: 928-936.

Miyasaki, K.T., Bodeau, A.L., Murthy, A.R., and Lehrer, R.I. (1993) *In vitro* antimicrobial activity of the human neutrophil cytosolic S-100 protein complex, calprotectin, against *Capnocytophaga sputigena*. *J Dent Res* **72**: 517-523.

Moreno, M.A., Ibrahim-Granet, O., Vicentefranqueira, R., Amich, J., Ave, P., Leal, F., *et al*. (2007) The regulation of zinc homeostasis by the ZafA transcriptional activator is essential for *Aspergillus fumigatus* virulence. *Mol Microbiol* **64**: 1182-1197.

Sambrook, J., and Russell, D.W., (2001) *Molecular Cloning. A laboratory manual*. Cold Spring Harbor Laboratory Press, Cold Spring, New York.

Sandrin, T.R., and Maier, R.M. (2003) Impact of metals on the biodegradation of organic pollutants. *Environ Health Perspect* **111**: 1093-1101.

Segurado, M., López-Aragon, R., Calera, J.A., Fernández-Abalos, J.M., and Leal, F. (1999) Zinc-regulated biosynthesis of immunodominant antigens from *Aspergillus spp*. *Infect Immun* **67**: 2377-2382.

Sheppard, D.C., Marr, K.A., Fredricks, D.N., Chiang, L.Y., Doedt, T., and Filler, S.G. (2006) Comparison of three methodologies for the determination of pulmonary fungal burden in experimental murine aspergillosis. *Clin Microbiol Infect* **12**: 376-380.

Smith, J.M., Davies, J.E., and Holden, D.W. (1993) Construction and pathogenicity of *Aspergillus fumigatus* mutants that do not produce the ribotoxin restrictocin. *Mol Microbiol* **9**: 1071-1077.

Sohnle, P.G., Hahn, B.L., and Santhanagopalan, V. (1996) Inhibition of *Candida albicans* growth by calprotectin in the absence of direct contact with the organisms. *J Infect Dis* **174**: 1369-1372.

Sohnle, P.G., Hunter, M.J., Hahn, B., and Chazin, W.J. (2000) Zinc-reversible antimicrobial activity of recombinant calprotectin (migration inhibitory factor-related proteins 8 and 14). *J Infect Dis* **182**: 1272-1275.

Spikes, S., Xu, R., Nguyen, C.K., Chamilos, G., Kontoyiannis, D.P., Jacobson, R.H., *et al*. (2008) Gliotoxin production in *Aspergillus fumigatus* contributes to host-specific differences in virulence. *J Infect Dis* **197**: 479-486.

Steinbakk, M., Naess-Andresen, C.F., Lingaas, E., Dale, I., Brandtzaeg, P., and Fagerhol, M.K. (1990) Antimicrobial actions of calcium binding leucocyte L1 protein, calprotectin. *Lancet* **336**: 763-765.

Stephens-Romero, S.D., Mednick, A.J., and Feldmesser, M. (2005) The pathogenesis of fatal outcome in murine pulmonary aspergillosis depends on the neutrophil depletion strategy. *Infect Immun* **73**: 114-125.

Striz, I., and Trebichavsky, I. (2004) Calprotectin - a pleiotropic molecule in acute and chronic inflammation. *Physiol Res* **53**: 245-253.

Taylor, K.M., and Nicholson, R.I. (2003) The LZT proteins; the LIV-1 subfamily of zinc transporters. *Biochim Biophys Acta* **1611**: 16-30.

Tekaia, F., and Latge, J.P. (2005) *Aspergillus fumigatus*: saprophyte or pathogen? *Curr Opin Microbiol* **8**: 385-392.

Urban, C.F., Ermert, D., Schmid, M., Abu-Abed, U., Goosmann, C., Nacken, W., *et al*. (2009) Neutrophil extracellular traps contain calprotectin, a cytosolic protein complex involved in host defense against *Candida albicans*. *PLoS Pathog* **5**: e1000639.

Vicentefranqueira, R., Moreno, M.A., Leal, F., and Calera, J.A. (2005) The *zrfA* and *zrfB* genes of *Aspergillus fumigatus* encode the zinc transporter proteins of a zinc uptake system induced in an acid, zinc-depleted environment. *Eukaryot Cell* **4**: 837-848.

Vogl, T., Leukert, N., Barczyk, K., Strupat, K., and Roth, J. (2006) Biophysical characterization of S100A8 and S100A9 in the absence and presence of bivalent cations. *Biochim Biophys Acta* **1763**: 1298-1306.

Weidner, G., d'Enfert, C., Koch, A., Mol, P.C., and Brakhage, A.A. (1998) Development of a homologous transformation system for the human pathogenic fungus *Aspergillus fumigatus* based on the *pyrG* gene encoding orotidine 5'-monophosphate decarboxylase. *Curr Genet* **33**: 378-385.

Yokus, B., and Cakir, U.D. (2006) Seasonal and physiological variations in serum chemistry and mineral concentrations in cattle. *Biol Trace Elem Res* **109**: 255-266.

ACKNOWLEDGMENTS

We wish to thank Belinda Rodriguez for her excellent technical assistance, Thomas Vogl (Institute of Immunology, Muenster, Germany) and Constantin F. Urban (Molecular Biology Department, Umeå University, Sweden) for providing plasmids for the expression of calprotectin and Mercedes Garayoa (Center for Cancer Research, Salamanca, Spain) for the meticulous examination of slices under the light microscope and photographic report. This work was supported by the Ministerio de Ciencia e Innovación (Spain) through grant BFU2010-22172/BMC to JAC and the ERA-NET Pathogenomics grant BFU2008-04709-E/BMC to EM. ARC was supported through the EYE/962/2010 training program in scientific research funded by the Junta de Castilla y León (Spain).

TABLES

Table 1. Fungal burden of lungs from leucopenic mice[1].

Strain	Genotype	CFU[2] (Mean ± SD)	GM[3] (Mean ± SD)	% Survival[4]
AF14	*wt*	9295 ± 3007	20.7 ± 5.2	0.0
AF54	Δ*zrfC*	7838 ± 6207	4.1 ± 3.8	23.8
AF731	Δ*zrfABC*[*zrfC*]	11850 ± 4988	28.1 ± 10.5	0.0
AF721	Δ*zrfABC*	161 ± 321	1.0 ± 1.7	76.9
AF791	Δ*zrfABC*[$zrfC^{\Delta N}$]	7658 ± 5654	10.4 ± 11.2	22.2

[1]Mice were euthanized to avoid suffering.

[2]Colony formation units per gram of lung tissue.

[3]Amount of galactomanan expressed as μg per gram of lung tissue.

[4]The correlations between survival and fungal burden were $r^2 = 0.959$ (for CFU, $P = 0.0006$) and $r^2 = 0.708$ (for GM, $P = 0.035$). Survival is that after 15 days post-infection.

Table 2. *Aspergillus fumigatus* strains used in this study.

Strain[1]	Detailed genotype[2]	Short genotype[2]	Reference
AF14	wild-type	wt	(Vicentefranqueira *et al*., 2005)
AF15	Δ*zrfA::neo* Δ*zrfB::hisG pyrG1* (PyrG$^-$)	Δ*zrfAB*	(Vicentefranqueira *et al*., 2005)
AF48*	Δ*zrfA::neo* Δ*zrfB::hisG*	Δ*zrfAB*	This study
AF52	Δ*zrfC::lacI pyrG1* (PyrG$^-$)	Δ*zrfC*	(Amich *et al.*, 2010)
AF54*	Δ*zrfC::lacI*	Δ*zrfC*	This study
AF2511	Δ*zrfA::neo* Δ*zrfB::hisG* Δ*zrfC::lacI pyrG1* (PyrG$^-$)	Δ*zrfABC*	(Amich *et al*., 2010)
AF721*	Δ*zrfA::neo* Δ*zrfB::hisG* Δ*zrfC::lacI*	Δ*zrfABC*	This study
AF731*	Δ*zrfA::neo* Δ*zrfB::hisG* Δ*zrfC::lacI* [*zrfC*]	Δ*zrfABC*[*zrfC*]	(Amich *et al*., 2010)
AF791*	Δ*zrfA::neo* Δ*zrfB::hisG* Δ*zrfC::lacI* [$zrfC^{\Delta 13\text{-}622}$]	Δ*zrfABC*[$zrfC^{\Delta N}$]	(Amich *et al*., 2010)
AF761*	Δ*zrfA::neo* Δ*zrfB::hisG*, Δ*zrfC::lacI* [*zrfB*]	Δ*zrfABC*[*zrfB*]	(Amich *et al*., 2010)
AF771*	Δ*zrfA::neo* Δ*zrfB::hisG* Δ*zrfC::lacI* [$zrfC^{P} \rightarrow zrfB^{cds}$]	Δ*zrfABC*[$C^{P} \rightarrow B^{cds}$]	This study
AF781*	Δ*zrfA::neo* Δ*zrfB::hisG* Δ*zrfC::lacI* [$zrfB^{P} \rightarrow zrfC^{cds}$]	Δ*zrfABC*[$B^{P} \rightarrow C^{cds}$]	This study
AF171*	Δ*zafA::hisG*	Δ*zafA*	(Moreno *et al*., 2007)

[1]Mutant strains labelled with an asterisk are isogenic to the wild-type strain for the *pyrG* gene.

[2]Genes in brackets were reintroduced into the *A. fumigatus* genome by targeting them at the intergenic region between the AFUA_2G08360 (*pyrG*) and AFUA_2G08350 genes.

FIGURE LEGENDS

Figure 1. Virulence of *A. fumigatus* strains. Survival of non-leucopenic mice (NL-mice) and leucopenic mice (L-mice) inoculated with 10^5 c/m of the wild-type, Δ*zrfC*, Δ*zrfABC* and Δ*zrfABC*[*zrfC*] strains. Each survival curve represents the combined results of two independent experiments (20 mice per strain). Survival curves were created with the Prism 4.0 Software, using the product-limit method of Kaplan-Meier, and were compared using the log-rank test. No statistically significant differences were observed between the survival of mice inoculated with the wild-type and Δ*zrfABC*[*zrfC*] revertant strain (AF14 ≈ AF731, $P = 0.099$ for NL-mice; $P = 0.892$ for L-mice). In contrast, highly statistically significant differences were observed between the survival of mice inoculated with the Δ*zrfC* and revertant or wild-type strains (AF54 > AF731 and AF54 > AF14, $P < 0.0001$ for both NL- and L-mice). Highly statistically significant differences were also observed between the survival of mice inoculated with the Δ*zrfC* and Δ*zrfABC* mutants (AF721 > AF54, $P < 0.0001$ for both NL- and L-mice).

Figure 2. Histopathological features of IPA in immunosuppressed mice. Sections of infected lungs from non-leucopenic mice (NL-mice, left panels) and leucopenic mice (L-mice, right panels) inoculated with the wild-type, Δ*zrfC*, Δ*zrfABC* and Δ*zrfABC*[*zrfC*] strains. The yellow arrowhead indicates a conidium germinating inside a macrophage. NL-mice inoculated with the wild-type, Δ*zrfC* and the Δ*zrfABC*[*zrfC*] revertant strain were euthanized after 7 days post-inoculation and after 15 days that inoculated with the Δ*zrfABC* strains. L-mice inoculated with the wild-type and revertant strains were euthanized after 4 days post-inoculation. L-mice inoculated with the Δ*zrfC* and Δ*zrfABC* strains were euthanized after 6 days post-inoculation. One lung from each euthanized mice was immediately excised and processed for histology. Tissues sections were stained with the GMS-HE stain. Hyphae appear as black filaments.

Pictures were taken with a 20× objective (except that for L-mice infected with the Δ*zrfABC* strain that was taken with a 100× objective). Bars = 50 μm.

Figure 3. Construction and phenotypic analysis of strains with exchanged coding sequences between the *zrfB* and *zrfC* genes. (A) Schematic representation of the construction of the derivative uridine-uracil-prototrophic $PyrG^{+}$ *A. fumigatus* strains that harbour either the coding sequence of *zrfB* under the control of the *zrfC* promoter (AF771, $zrfC^{P}\rightarrow zrfB^{cds}$) or the coding sequence of *zrfC* under the control of the *zrfB* promoter (AF781, $zrfB^{P}\rightarrow zrfC^{cds}$) inserted between the AFUA_2G08360 (*pyrG*) and AFUA_2G08350 loci of the AF2511 uridine-uracil-auxotrophic *pyrG1* strain. **(B)** Transcriptional analysis by northern blot of the *zrfB* and *zrfC* genes in the strains AF771 and AF781 cultured in the acidic (SDA–Zn, pH 4.5) and alkaline (SDN–Zn, pH 7.5) zinc-limiting media for 20 hours at 37ºC. The expression of these genes was also analysed in the AF761 Δ*zrfABC*[*zrfB*] and AF731 Δ*zrfABC*[*zrfC*] strains as controls. The 5'-UTR regions of *zrfB* and *zrfC* have approximately 268 and 32 nucleotides, respectively (Vicentefranqueira *et al*., 2005; Amich *et al*., 2010). The size of transcripts is indicated in kb. The size of the *zrfB* transcript synthesized by the AF771 strain was lower than the wild-type *zrfB* transcript synthesized by AF761 because the former has the 5'-UTR region of *zrfC*, which is ~236 nucleotides shorter than the 5'-UTR of *zrfB*. In contrast, the size of the *zrfC* transcript synthesized by the AF781 strain was bigger than the wild-type *zrfC* transcript synthesized by AF731 because the former carries the 5'-UTR region of *zrfB*, which is ~236 nucleotides longer than the 5'-UTR of *zrfC*. **(C)** Growth capacity of the AF771 and AF781 strains cultured on acidic (SDAE–Zn, pH 4.5) and alkaline (SDNE–Zn, pH 7.5) agar media supplemented with increasing amounts of Zn^{2+} (0-1000 μM). The AF761 and AF731 were included as controls. It could be possible that the 5'-UTR region of *zrfB* and/or *zrfC* in the chimerical $zrfB^{P}\rightarrow zrfC^{cds}$ and $zrfC^{P}\rightarrow zrfB^{cds}$ genes somehow interfere with the translation of the ZrfC and ZrfB proteins,

respectively. However, this is unlikely as these 5'-UTRs lack alternative AUGs or any other known feature that could interfere with translation. The SDAE and SDNE agar plates inoculated with conidia were incubated at 37ºC for 5 and 3 days, respectively, before pictures were taken.

Figure 4. Function of the N-terminus of ZrfC in virulence. (A) Survival of leucopenic mice (L-mice) inoculated with 10^4 conidia per mouse (open black symbols) of the wild-type, Δ*zrfC*, Δ*zrfABC*, Δ*zrfABC*[*zrfC*] and Δ*zrfABC*[$zrfC^{\Delta N}$] strains and 10^5 c/m of the Δ*zrfABC*[$zrfC^{\Delta N}$] strain (closed red symbols). The survival of L-mice inoculated with 10^5 c/m of the Δ*zrfC* strain (closed blue symbols) showed in figure 1 was also represented here for comparison purposes. Each survival curve represents the combined results of two independent experiments (20 mice per strain). Survival curves were created with the Prism 4.0 Software, using the product-limit method of Kaplan-Meier, and were compared using the log-rank test. No statistically significant differences were observed between the survival of L-mice inoculated with 10^4 c/m of the wild-type and Δ*zrfABC*[*zrfC*] revertant strain (AF14 ≈ AF731, $P = 0.838$), between the survival of L-mice inoculated with 10^4 c/m of the Δ*zrfC* and Δ*zrfABC*[$zrfC^{\Delta N}$] strain (AF54 ≈ AF791, $P = 0.925$) and between the survival of L-mice inoculated with 10^5 c/m of the Δ*zrfC* and Δ*zrfABC*[$zrfC^{\Delta N}$] strain (AF54 ≈ AF791, $P = 0.791$). In contrast, highly statistically significant differences were observed between the survival of L-mice inoculated with 10^4 c/m of the Δ*zrfC* and revertant or wild-type strain (AF54 > AF14 and AF54 > AF731, $P = 0.001$), between the survival of L-mice inoculated with the Δ*zrfABC* and Δ*zrfC* or Δ*zrfABC*[$zrfC^{\Delta N}$] strain (AF721 > AF54 and AF721 > AF791, $P < 0.003$) and between the survival rate of L-mice inoculated with the Δ*zrfABC*[$zrfC^{\Delta N}$] and Δ*zrfABC*[*zrfC*] strain (AF791 > AF731, $P = 0.008$). **(B)** Histopathological features of lung sections from infected L-mice inoculated with 10^4 c/m of the wild-type, Δ*zrfC*, Δ*zrfABC*[$zrfC^{\Delta N}$] and Δ*zrfABC*[*zrfC*] strains. All mice were euthanized after

5 days post-inoculation. Tissue sections were stained with GMS-HE. Pictures were taken with a 10× objective. Bar = 50 μm.

Figure 5. Immunolocalization and quantification of calprotectin in lungs of immunosuppressed mice. Non-inoculated (NI panels), non-leucopenic and leucopenic mice (NL- and L-mice) and NL- and L-mice inoculated (I panels) with a Δ*zrfABC*[*zrfC*] strain (10^5 c/m) were sacrificed after 4 days post-infection. Consecutive lung sections were stained with the GMS-HE stain and immunocytochemically with a goat antibody against the A subunit of mouse calprotectin (α-CalA). The insets in the NI panels show in more detail the immunostained calprotectin in neutrophils that are not observed at low magnification. Lung sections from mice infected with the Δ*zrfABC*[*zrfC*] strain were also stained immunocytochemically with a goat isotype antibody as a control for the α-CalA antibody specificity. The percent area of immunostained calprotectin (ISCP), which can be located in patches and/or within scattered neutrophils, was measured in the lung sections of five mice per condition using the ImageJ software. The percent areas of ISCP in NL- and L-mice were represented and analysed statistically with the Prism 4.0 Software using the two-tailed, unpaired t-test. Only significant differences were indicated with asterisks (**$P < 0.001$, ***$P < 0.0001$). The increase ratios between the average percent area measured in lung sections of inoculated (I) and non-inoculated mice (NI) immunostained with the α-CalA antibody are compiled in a little table. Pictures were taken with a 4× objective except those in the insets that were taken with a 20× objective. Bar = 1 mm (in the inset = 100 μm).

Figure 6. Inhibition of fungal growth *in vitro* by calprotectin. The wild-type, Δ*zrfC*, Δ*zrfA*Δ*zrfB*Δ*zrfC* and Δ*zrfA*Δ*zrfBzrfC*$^{+}$ strains were cultured in the SDN medium containing 2 μM rhCP (+) or just buffer (–) in Mn-replete **(A)** and Mn-limiting media **(B)** with or without a supplement of zinc. The Zn-replete and/or Mn-replete conditions were achieved by supplementing the medium with 4 μM Zn^{2+} and/or 2.0 μM Mn^{2+}, respectively. The relative net fungal growth of all strains was normalized to the net fungal growth reached by the wild-type strain cultured in SDN+Zn+Mn in the absence of calprotectin (i.e. 3.733 ± 0.246 mg/mL). All data represent the average of two independent experiments with three replicates for each strain and assayed condition. Graphics were created and data analysed statistically with the Prism 4.0 Software using the two-tailed, unpaired t-test. Only significant differences were indicated with asterisks (*$P < 0.05$, **$P < 0.001$ or ***$P < 0.0001$).

SUPPLEMENTARY FIGURE LEGENDS

Figure S1. Virulence of a Δ*zrfA*Δ*zrfB* strain. Survival of leucopenic mice inoculated with 10^5 c/m of the Δ*zrfAB* and Δ*zrfABC*[*zrfC*] strains. Each survival curve represents the combined results of two independent experiments (20 mice per strain). Survival curves were created with the Prism 4.0 Software, using the product-limit method of Kaplan-Meier, and were compared using the log-rank test. No statistically significant differences were observed between mice survival (AF48 ≈ AF731, $P = 0.485$).

Figure S2. Germination rate of conidia *in vitro*. The germination rates of the wild-type, Δ*zrfC*, Δ*zrfABC* and Δ*zrfABC*[*zrfC*] conidia were measured both in the alkaline SDN zinc-limiting medium (pH 7.5) and in the BSD50 medium (pH 7.5). The germination rate of Δ*zafA* conidia, which have a defect in germination under acidic zinc-limiting conditions (Moreno et al., 2007), was also measured in these media. Conidial germination was followed by microscopic observations of culture samples taken after 5, 6, 7, 8, 9 and 10 hours of incubation in liquid media inoculated to a density of 5×10^5 spores/mL and incubated at 37°C with shaking at 200 rpm. It was considered that a conidium had germinated when the length of the germ tube reached at least half of the diameter of a swollen conidium. To obtain more accurate counts of germinated conidia, aggregates were dispersed by sonication before they were counted on a haemocytometer. No changes in the germination rates were observed after 8 hours. All strains exhibited germination rates >95% in the BSD50 medium, which provided a good control for conidial viability. The germination rates were expressed as the mean ± standard error of the mean (SEM) from three independent experiments, each with three independent counts for each strain and time-point. Graphics were created and data analyzed statistically with the Prism 4.0 Software, using a two-way ANOVA test followed by a Bonferroni post-test with the wild-type

germination rate as reference. Asterisks indicate a significance of $P < 0.05$ (*) or $P < 0.001$ (**); ns, not significant. The box at the bottom of the figure shows the color code used to identify the fungal strain.

Figure S3. Growth of fungal strains used in virulence studies. (A) Growth of the wild-type, Δ*zrfC*, Δ*zrfAB*, Δ*zrfABC*, Δ*zrfABC*[*zrfC*] and Δ*zrfABC*[$zrfC^{\Delta N}$] strains onto acidic (SDAE–Zn, pH 4.5) and alkaline (SDNE–Zn, pH 7.5) agar supplemented with increasing amounts of Zn^{2+} (0-1000 μM). **(B)** Growth of the same strains onto alkaline BSD10 and BSD50 agar (pH 7.5) and in these media with a supplement of 100 and 1000 μM Zn^{2+}. All plates were spotted with 10^3 conidia per strain. The BSD10 and SDNE agar plates were incubated for three days at 37ºC before pictures were taken. The BSD50 and SDAE agar plates were incubated for five days.

Figure S4. Comparison of the effect of the *zrfB* and $zrfC^{\Delta N}$ genes on fungal growth under alkaline zinc-limiting conditions. The Δ*zrfABC*[$zrfC^{\Delta N}$] and Δ*zrfABC*[$C^{P} \rightarrow B^{cds}$] strains were cultured onto alkaline agar (SDNE–Zn, pH 7.5) supplemented with increasing amounts of Zn^{2+} (0-1000 μM). Note that the *zrfC* promoter drives the expression of both the $zrfC^{\Delta N}$ and *zrfB* coding sequences in AF791 and AF771, respectively. The Δ*zrfABC*[*zrfC*] and Δ*zrfABC*[*zrfB*] strains were included as controls. The SDNE agar plates were spotted with 10^3 conidia per strain and incubated at 37ºC in a humid atmosphere for three days, respectively, before pictures were taken.

Figure S5. Effect of manganese on the growth ability of a Δ*zrfC* mutant depending on zinc availability. The Δ*zrfC* and wild-type strains were cultured onto alkaline manganese/zinc-limiting agar (i.e. SDN–Mn–Zn plus 250 μM EDTA and solidified with 2% agar, pH 7.2) supplemented with increasing amounts of Zn^{2+} (0-1000 μM) and 2 μM Mn^{2+} (+Mn) or without

Mn^{2+} (–Mn). Plates were spotted with 10^3 conidia per strain and incubated at 37ºC in a humid atmosphere for three days before pictures were taken. As shown, the growth capacity of a Δ*zrfC* strain is not affected apparently under Mn-limiting conditions regardless of zinc availability.

Figure S6. Relative expression measured by quantitative real-time PCR (qRT-PCR) of *zrfA* and *zrfB* in a Δ*zrfC* strain and of *zrfC* in a Δ*zrfA*Δ*zrfB* strain compared to a wild-type strain. All strains were cultured for 20 hours at 37ºC in the alkaline SDN zinc-limiting medium without a zinc supplement (–Zn) and supplemented with 2 and 100 μM Zn^{2+}. Total RNA was purified with the RNeasy Plant kit (Qiagen) and treated with DNase I RNase-free (Invitrogen) to remove genomic DNA. DNase-treated RNA (12 μg) was used to synthesize cDNA at 50ºC for 90 min using the SuperScript III RNase $H^–$Reverse Transcriptase (Invitrogen) and oligo dT_{15} (Roche) as primers. qRT-PCR was done using the SsoAdvanced SYBR Green supermix (Bio-Rad) and the primers ZRFA-D and ZRFA-R for *zrfA*, ZRFB-D and ZRFB-R for *zrfB*, and ZRFC-D and ZRFC-R for *zrfC* (**Table S1**). The CFX96 Touch Real-Time PCR Detection System (Bio-Rad) was used with the following program: initial denaturation at 95ºC for 8 min following by 40 cycles of 95ºC for 15 s, 59ºC for 30 s and 72ºC for 10 s. The expression of the *zrfA*, *zrfB* and *zrfC* genes was measured in triplicate for two independent cDNA samples from each strain and culture condition. Amplification specificity was determined by meelting curve analysis. Data were normalized using the *gdpA* and *tubA* genes as internal references **(Table S1)**. The $2^{-\Delta\Delta Ct}$ method was used to measure the relative expression level of the genes in the AF48 (Δ*zrfAB*) and AF54 (Δ*zrfC*) strains compared to that in the AF14 (wild-type) strain. Data were represented and analyzed statistically with the Prism 4.0 Software. The reference expression level for all genes in the wild-type strain is indicated by a dotted line. As expected, the expression of *zrfA* and *zrfB* in the Δ*zrfAB* strain and *zrfC* in the Δ*zrfC* strain were not detected by qRT-PCR. Nevertheless, near-zero relative expression values have been

represented to allow the readers to observe their places in the graph (#). Statistical analysis was performed using a two-way ANOVA test followed by a Bonferroni post-test with the wild-type expression level as reference. Significant differences were detected for the expression of both *zrfA* and *zrfB* between the wild-type and Δ*zrfC* strains (AF14 < AF54, $P = 0.001$).

SUPPLEMENTARY TABLE

Table S1. Oligonucleotides used in quantitative real-time PCR (qRT-PCR).

Gene	Name	5′-Sequence-3′
zrfA (AFUA_1G01550)	JA43-D	ATGCTCAAGCCCGCACGAATC
	JA13-R	ATGCCGAATTCGAGGATCAGG
zrfB (AFUA_2G03860)	ZRFB-D	ACCGGCAGAAGAAGCATTGA
	ZRFB-R	ACCGCATCACCATCAACTCA
zrfC (AFUA_4G09560)	ZRFC-D	CAAACTCTCGGTGCTCGTCA
	ZRFC-R	GAAGACAATCACCACCAGCA
tubA (AFUA_1G10910)	BTUB-D	AACAACATCCAGACCGCTCT
	BTUB-R	TGATCACCGACACGCTTGAA
gdpA (AFUA_5G01970)	GDPA-D	AGTTCGGCATTGTTGAGGGT
	GDPA-R	TGATGTTCTGGGCAGCAGTA

Figure 1

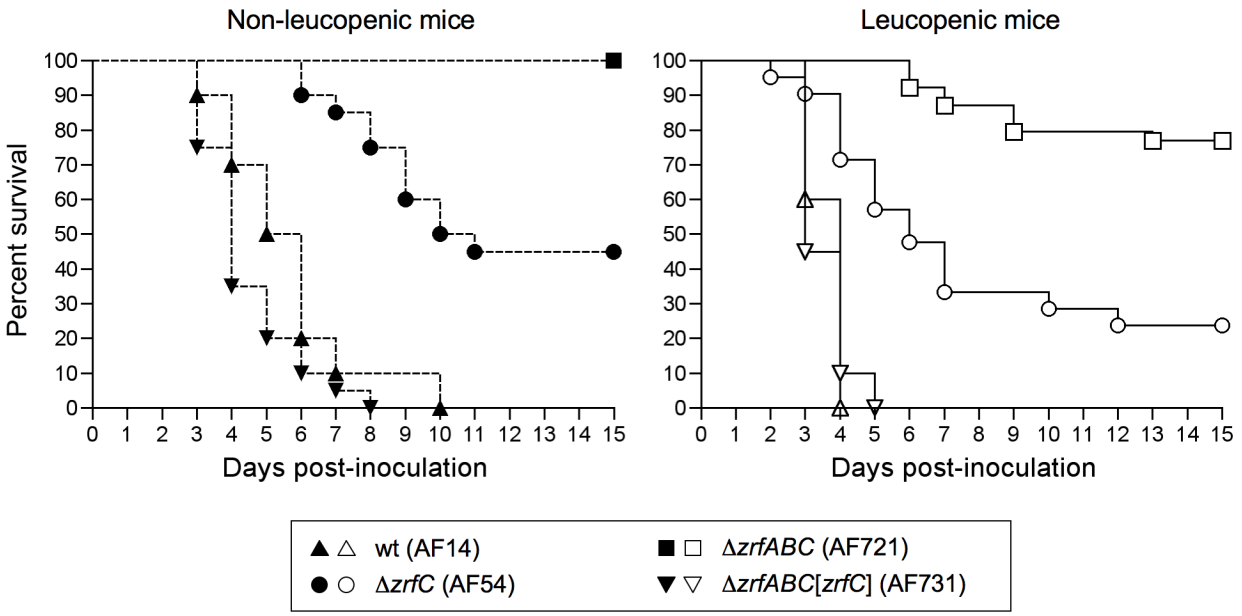
Non-leucopenic mice
Leucopenic mice
Percent survival
Days post-inoculation
Days post-inoculation
▲ △ wt (AF14)
■ □ ΔzrfABC (AF721)
● ○ ΔzrfC (AF54)
▼ ▽ ΔzrfABC[zrfC] (AF731)

Figure 2

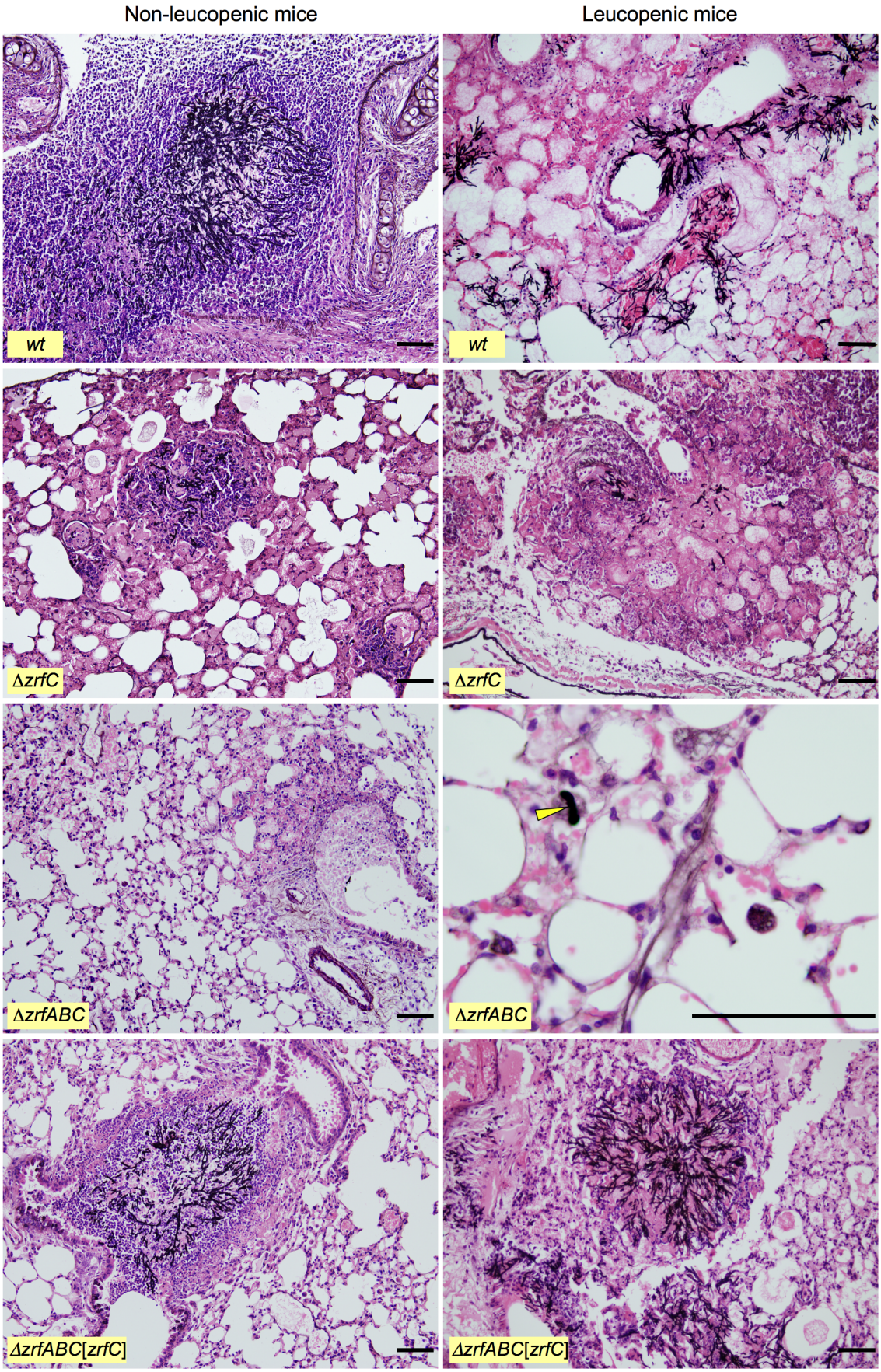
Non-leucopenic mice
Leucopenic mice
wt
wt
ΔzrfC
ΔzrfC
ΔzrfABC
ΔzrfABC
ΔzrfABC[zrfC]
ΔzrfABC[zrfC]

Figure 3

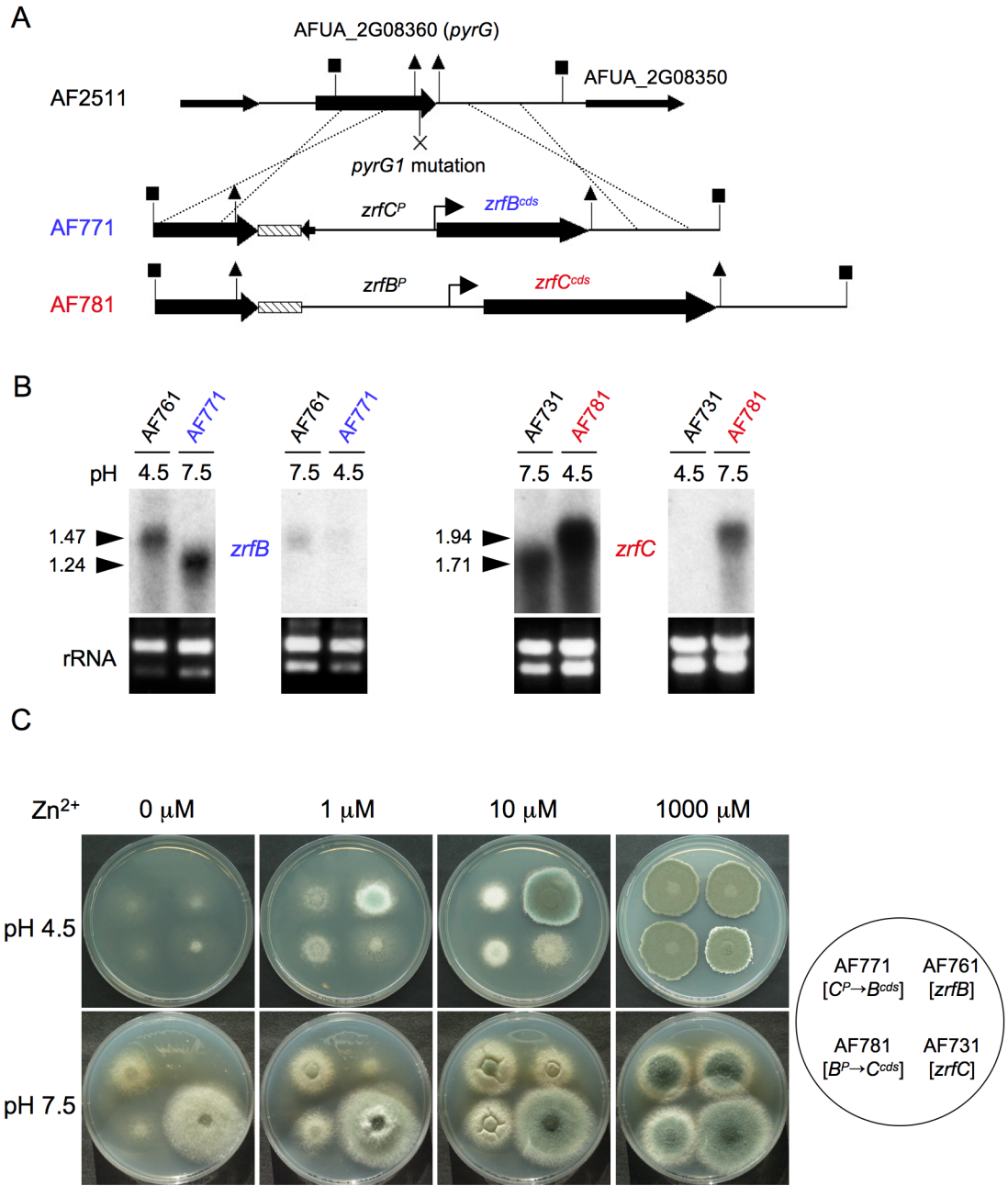
A
AFUA_2G08360 (pyrG)
AFUA_2G08350
AF2511
pyrG1 mutation
AF771
zrfC^P
zrfB^cds
AF781
zrfB^P
zrfC^cds
B
AF761
AF771
AF731
AF781
pH
4.5
7.5
1.47
1.24
zrfB
1.94
1.71
zrfC
rRNA
C
Zn2+
0 μM
1 μM
10 μM
1000 μM
pH 4.5
pH 7.5
AF771 [C^P→B^cds]
AF761 [zrfB]
AF781 [B^P→C^cds]
AF731 [zrfC]

Figure 4

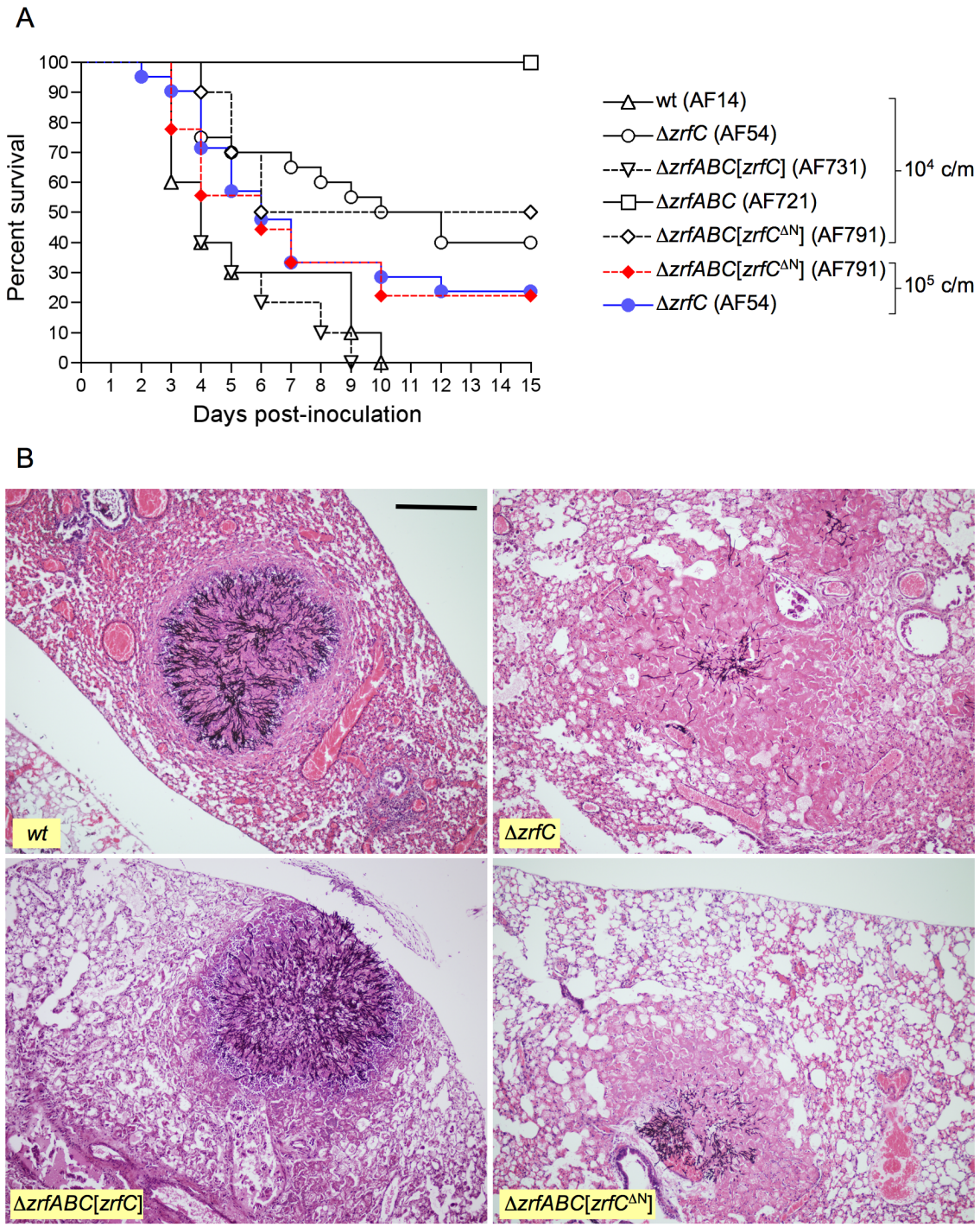
A
Percent survival
Days post-inoculation
wt (AF14)
ΔzrfC (AF54)
ΔzrfABC[zrfC] (AF731)
ΔzrfABC (AF721)
ΔzrfABC[zrfCΔN] (AF791)
ΔzrfABC[zrfCΔN] (AF791)
ΔzrfC (AF54)
10^4 c/m
10^5 c/m
B
wt
ΔzrfC
ΔzrfABC[zrfC]
ΔzrfABC[zrfCΔN]

Figure 5

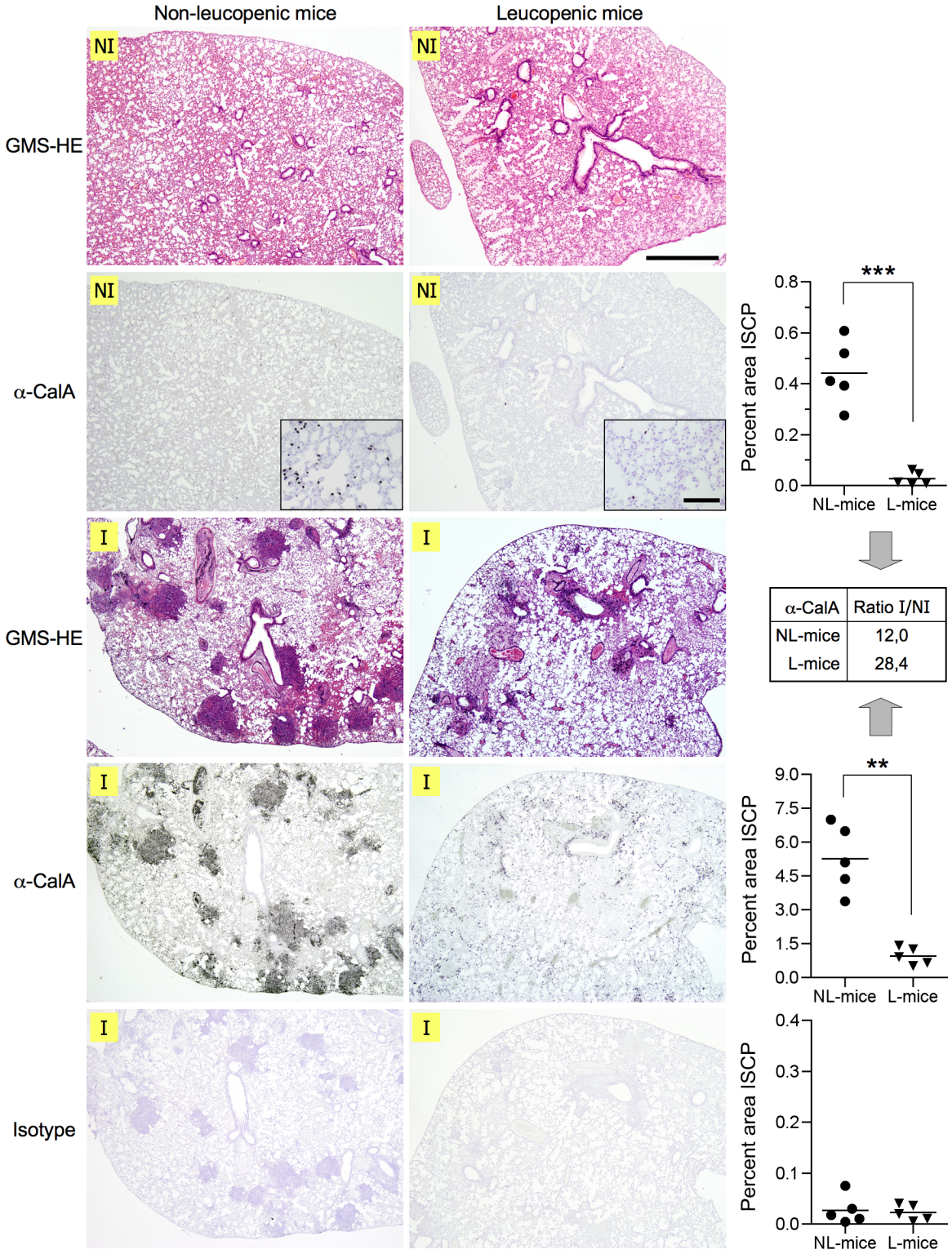
Non-leucopenic mice
Leucopenic mice
GMS-HE
α-CalA
GMS-HE
α-CalA
Isotype
NI
I
Percent area ISCP
***
**
NL-mice
L-mice
α-CalA
Ratio I/NI
NL-mice
12,0
L-mice
28,4

Figure 6

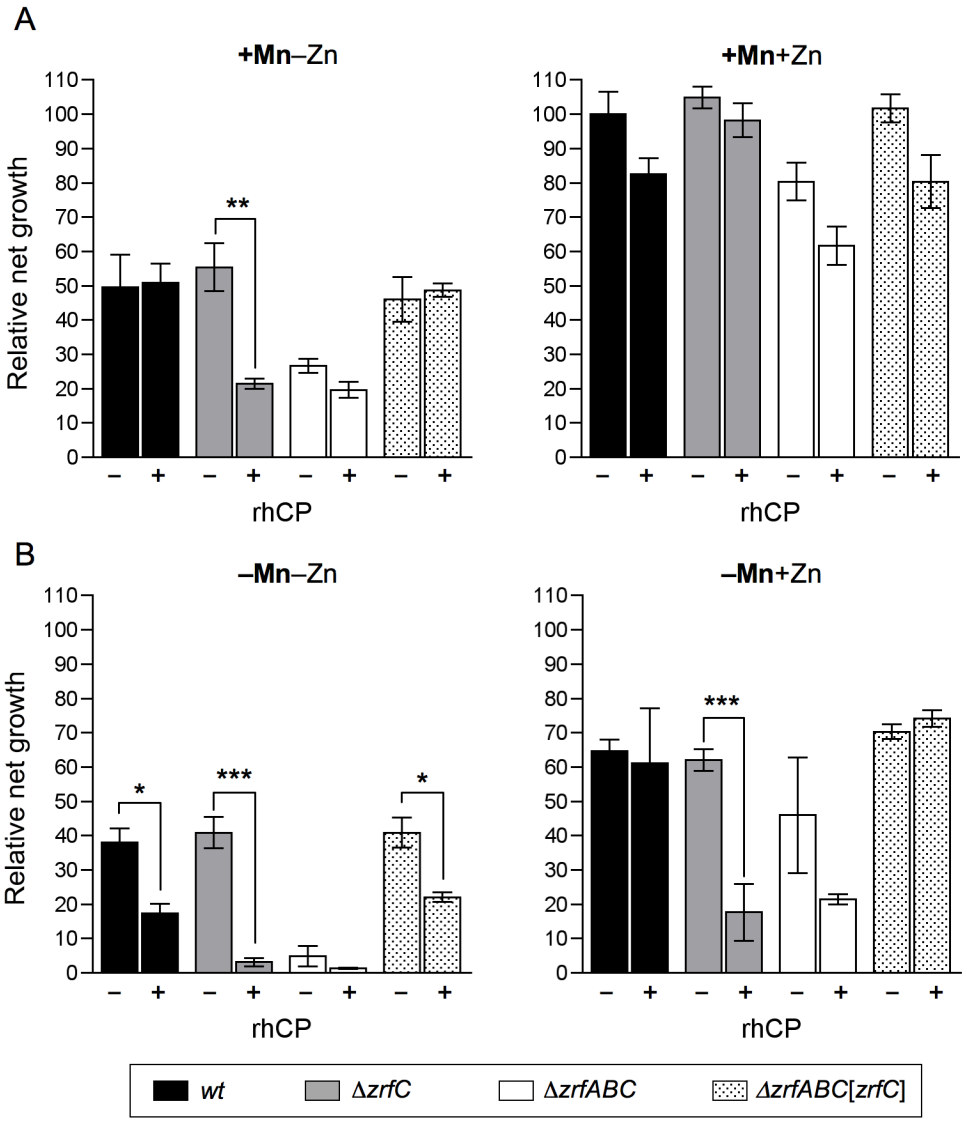
A
+Mn–Zn
+Mn+Zn
Relative net growth
rhCP
B
–Mn–Zn
–Mn+Zn
wt
ΔzrfC
ΔzrfABC
ΔzrfABC[zrfC]

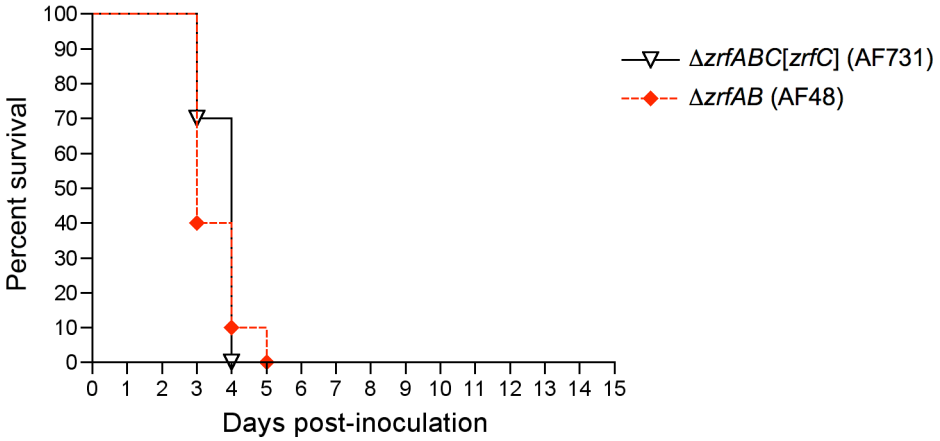

Figure S1. Virulence of a Δ*zrfA*Δ*zrfB* strain. Survival of leucopenic mice inoculated with 10^5 c/m of the Δ*zrfAB* and Δ*zrfABC*[*zrfC*] strains. Each survival curve represents the combined results of two independent experiments (20 mice per strain). Survival curves were created with the Prism 4.0 Software, using the product-limit method of Kaplan-Meier, and were compared using the log-rank test. No statistically significant differences were observed between mice survival (AF48 ≈ AF731, $P = 0.485$).

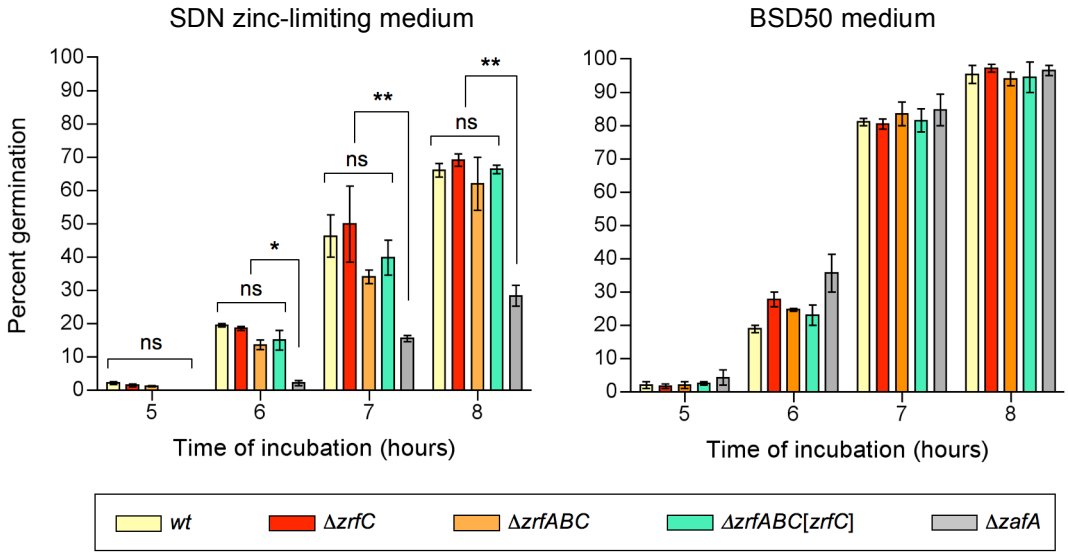

Figure S2. Germination rate of conidia *in vitro*. The germination rates of the wild-type, Δ*zrfC*, Δ*zrfABC* and Δ*zrfABC*[*zrfC*] conidia were measured both in the alkaline SDN zinc-limiting medium (pH 7.5) and in the BSD50 medium (pH 7.5). The germination rate of Δ*zafA* conidia, which have a defect in germination under acidic zinc-limiting conditions (Moreno et al., 2007), was also measured in these media. Conidial germination was followed by microscopic observations of culture samples taken after 5, 6, 7, 8, 9 and 10 hours of incubation in liquid media inoculated to a density of 5×10^5 spores/mL and incubated at 37°C with shaking at 200 rpm. It was considered that a conidium had germinated when the length of the germ tube reached at least half of the diameter of a swollen conidium. To obtain more accurate counts of germinated conidia, aggregates were dispersed by sonication before they were counted on a haemocytometer. No changes in the germination rates were observed after 8 hours. All strains exhibited germination rates >95% in the BSD50 medium, which provided a good control for conidial viability. The germination rates were expressed as the mean ± standard error of the mean (SEM) from three independent experiments, each with three independent counts for each strain and time-point. Graphics were created and data analyzed statistically with the Prism 4.0 Software, using a two-way ANOVA test followed by a Bonferroni post-test with the wild-type germination rate as reference. Asterisks indicate a significance of $P < 0.05$ (*) or $P < 0.001$ (**); ns, not significant. The box at the bottom of the figure shows the color code used to identify the fungal strain.

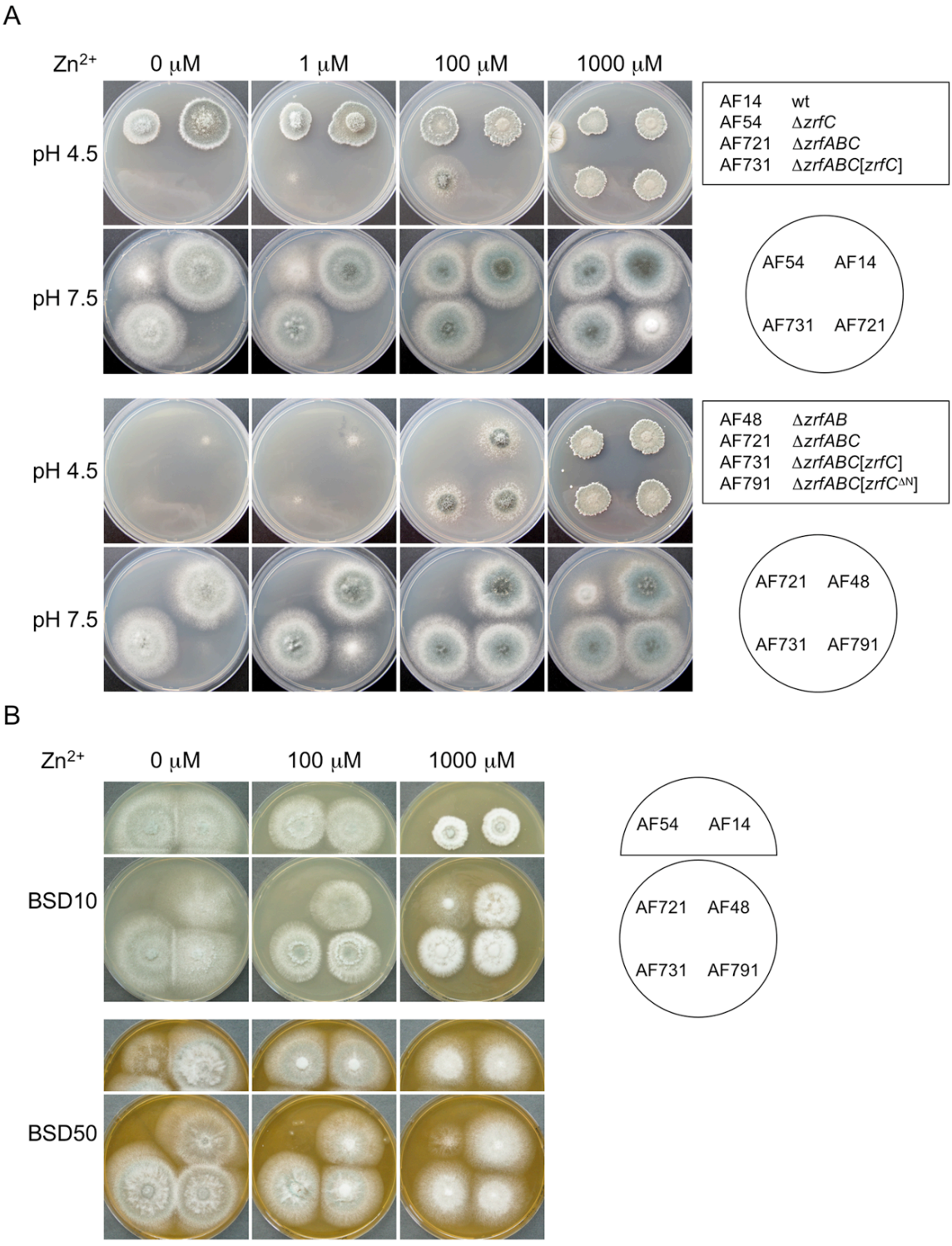

Figure S3. Growth of fungal strains used in virulence studies. (A) Growth of the wild-type, Δ*zrfC*, Δ*zrfAB*, Δ*zrfABC*, Δ*zrfABC*[*zrfC*] and Δ*zrfABC*[$zrfC^{\Delta N}$] strains onto acidic (SDAE–Zn, pH 4.5) and alkaline (SDNE–Zn, pH 7.5) agar supplemented with increasing amounts of Zn^{2+} (0-1000 μM). **(B)** Growth of the same strains onto alkaline BSD10 and BSD50 agar (pH 7.5) and in these media with a supplement of 100 and 1000 μM Zn^{2+}. All plates were spotted with 10^3 conidia per strain. The BSD10 and SDNE agar plates were incubated for three days at 37ºC before pictures were taken. The BSD50 and SDAE agar plates were incubated for five days.

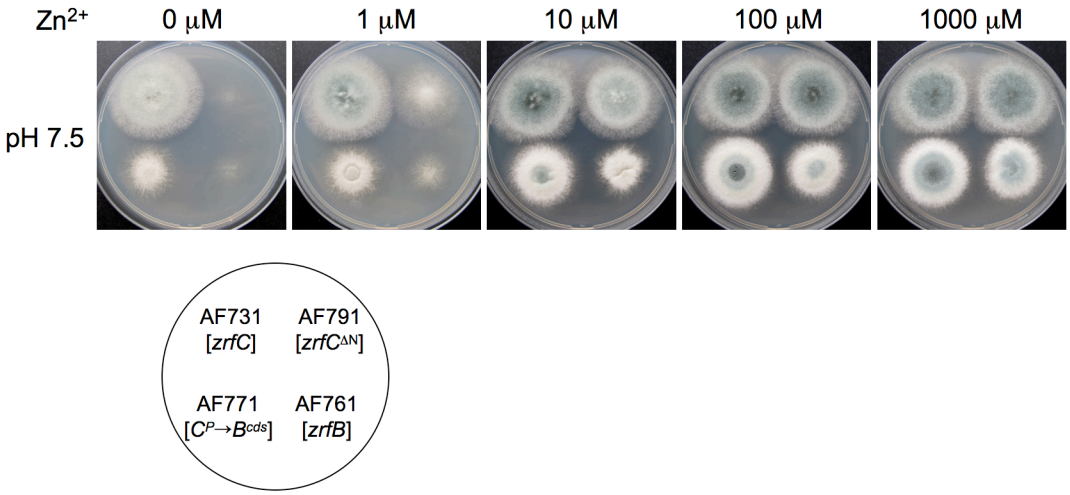

Figure S4. Comparison of the effect of the *zrfB* and *zrfC*$^{\Delta N}$ genes on fungal growth under alkaline zinc-limiting conditions. The Δ*zrfABC*[*zrfC*$^{\Delta N}$] and Δ*zrfABC*[*C*^{P}→*B*^{cds}] strains were cultured onto alkaline agar (SDNE–Zn, pH 7.5) supplemented with increasing amounts of Zn^{2+} (0-1000 μM). Note that the *zrfC* promoter drives the expression of both the *zrfC*$^{\Delta N}$ and *zrfB* coding sequences in AF791 and AF771, respectively. The Δ*zrfABC*[*zrfC*] and Δ*zrfABC*[*zrfB*] strains were included as controls. The SDNE agar plates were spotted with 10^3 conidia per strain and incubated at 37ºC in a humid atmosphere for three days, respectively, before pictures were taken.

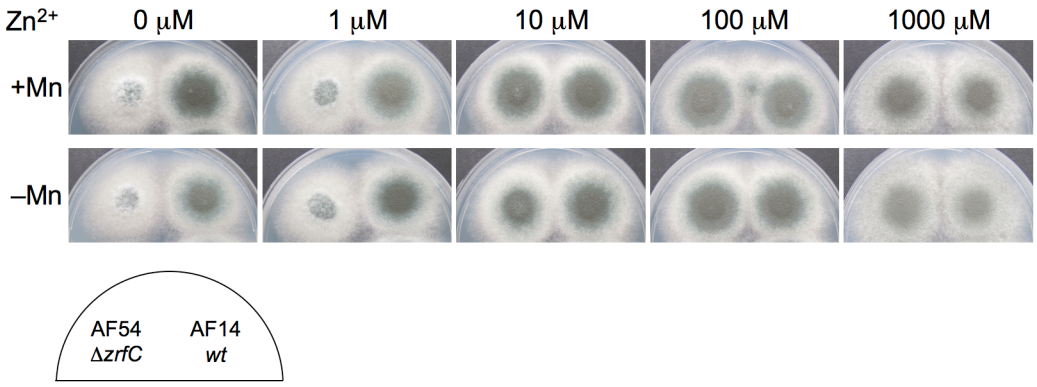

Figure S5. Effect of manganese on the growth ability of a Δ*zrfC* mutant depending on zinc availability. The Δ*zrfC* and wild-type strains were cultured onto alkaline manganese/zinc-limiting agar (i.e. SDN–Mn–Zn plus 250 μM EDTA and solidified with 2% agar, pH 7.2) supplemented with increasing amounts of Zn^{2+} (0-1000 μM) and 2 μM Mn^{2+} (+Mn) or without Mn^{2+} (–Mn). Plates were spotted with 10^3 conidia per strain and incubated at 37ºC in a humid atmosphere for three days before pictures were taken. As shown, the growth capacity of a Δ*zrfC* strain is not affected apparently under Mn-limiting conditions regardless of zinc availability.

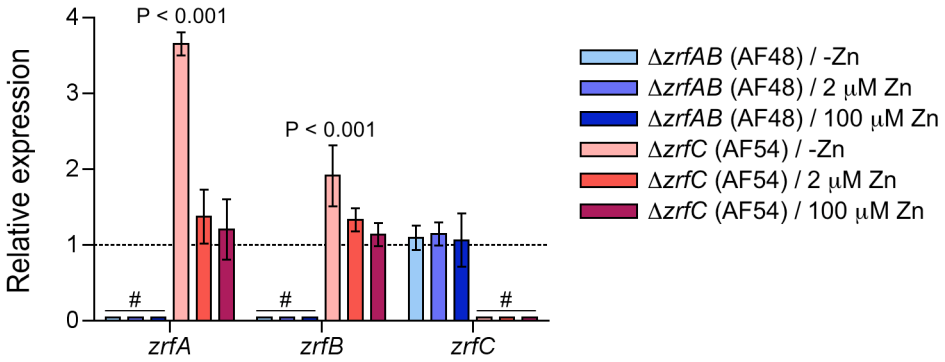

Figure S6. Relative expression measured by quantitative real-time PCR (qRT-PCR) of *zrfA* and *zrfB* in a Δ*zrfC* strain and of *zrfC* in a Δ*zrfA*Δ*zrfB* strain compared to a wild-type strain. All strains were cultured for 20 hours at 37ºC in the alkaline SDN zinc-limiting medium without a zinc supplement (–Zn) and supplemented with 2 and 100 μM Zn^{2+}. Total RNA was purified with the RNeasy Plant kit (Qiagen) and treated with DNase I RNase-free (Invitrogen) to remove genomic DNA. DNase-treated RNA (12 μg) was used to synthesize cDNA at 50ºC for 90 min using the SuperScript III RNase H⁻Reverse Transcriptase (Invitrogen) and oligo dT_{15} (Roche) as primers. qRT-PCR was done using the SsoAdvanced SYBR Green supermix (Bio-Rad) and the primers ZRFA-D and ZRFA-R for *zrfA*, ZRFB-D and ZRFB-R for *zrfB*, and ZRFC-D and ZRFC-R for *zrfC* (**Table S1**). The CFX96 Touch Real-Time PCR Detection System (Bio-Rad) was used with the following program: initial denaturation at 95ºC for 8 min following by 40 cycles of 95ºC for 15 s, 59ºC for 30 s and 72ºC for 10 s. The expression of the *zrfA*, *zrfB* and *zrfC* genes was measured in triplicate for two independent cDNA samples from each strain and culture condition. Amplification specificity was determined by meelting curve analysis. Data were normalized using the *gdpA* and *tubA* genes as internal references **(Table S1)**. The $2^{-\Delta\Delta Ct}$ method was used to measure the relative expression level of the genes in the AF48 (Δ*zrfAB*) and AF54 (Δ*zrfC*) strains compared to that in the AF14 (wild-type) strain. Data were represented and analyzed statistically with the Prism 4.0 Software. The reference expression level for all genes in the wild-type strain is indicated by a dotted line. As expected, the expression of *zrfA* and *zrfB* in the Δ*zrfAB* strain and *zrfC* in the Δ*zrfC* strain were not detected by qRT-PCR. Nevertheless, near-zero relative expression values have been represented to allow the readers to observe their places in the graph (#). Statistical analysis was performed using a two-way ANOVA test followed by a Bonferroni post-test with the wild-type expression level as reference. Significant differences were detected for the expression of both *zrfA* and *zrfB* between the wild-type and Δ*zrfC* strains (AF14 < AF54, $P = 0.001$).

Table S1. Oligonucleotides used in quantitative real-time PCR (qRT-PCR).

Gene	Name	5´-Sequence-3´
zrfA (AFUA_1G01550)	ZRFA-D	ATGCTCAAGCCCGCACGAATC
	ZRFA-R	ATGCCGAATTCGAGGATCAGG
zrfB (AFUA_2G03860)	ZRFB-D	ACCGGCAGAAGAAGCATTGA
	ZRFB-R	ACCGCATCACCATCAACTCA
zrfC (AFUA_4G09560)	ZRFC-D	CAAACTCTCGGTGCTCGTCA
	ZRFC-R	GAAGACAATCACCACCAGCA
tubA (AFUA_1G10910)	BTUB-D	AACAACATCCAGACCGCTCT
	BTUB-R	TGATCACCGACACGCTTGAA
gdpA (AFUA_5G01970)	GDPA-D	AGTTCGGCATTGTTGAGGGT
	GDPA-R	TGATGTTCTGGGCAGCAGTA